Chemistry and Physics of Lipids 221 (2019) 128–139

Contents lists available at ScienceDirect

Chemistry and Physics of Lipids

journal homepage: www.elsevier.com/locate/chemphyslip

Locating intercalants within lipid bilayers using fluorescence quenching by bromophospholipids and iodophospholipids

Carmit Alexenberg, Michal Afri, Shlomi Eliyahu, Hani Porat, Ayala Ranz, Aryeh A. Frimer*

The Department of Chemistry, Bar-Ilan University, Ramat Gan, 5290002, Israel

ARTICLE INFO

Keywords:
DMPC liposomes
Bioliposomes
Erythrocyte ghosts
Bromophospholipid
Iodophospholipid
Fluorescence quenching
Intercalant depth
Porphyrins

ABSTRACT

In previous work, we have been able to determine the depth of intercalated molecules within the lipid bilayer using the solvent polarity sensitivity of three spectroscopic techniques: the ^{13}C NMR chemical shift (δ); the fluorescence emission wavelength (λ_{em}), and the ESR β-H splitting constants ($a_{\beta\text{-}H}$). In the present paper, we use the quenching by a heavy atom (Br or I), situated at a known location along a phospholipid chain, as a probe of the location of a fluorescent moiety. We have synthesized various phospholipids with bromine (or iodine) atoms substituted at various locations along the lipid chain. The latter halolipids were intercalated in turn with various fluorophores into DMPC liposomes, biomembranes and erythrocyte ghosts. The most effective fluorescence quenching occurs when the heavy atom location corresponds to that of the fluorophore. The results show that generally speaking the fluorophore intercalates the same depth independent of which lipid bilayer is used. KBr (or KI) is the most effective quencher when the fluorophore resides in or at the aqueous phase. Presumably because of iodine's larger radius and spin coupling constant, the iodine analogs are far less discriminating in the depth range it quenches.

1. Introduction

The cell membrane plays a crucial role in protecting the cell from pathological agents by modulating the crossing of chemicals into and out of the cell. While previous research has focused largely on the aqueous phase of the cell, there is now increasing interest in the lipophilic phase, i.e., within the membrane itself. Over the past two decades, we have focused our studies primarily on the hydrophobic phospholipid bilayers of DMPC liposomes, which serve as a simple model for biological membranes (Gregoriadis, 1984; Papahadjopoulos, 1978). In our previous work, we have been able to determine the depth of intercalated molecules (henceforth, intercalants) within the lipid bilayer using three different spectroscopic techniques: **NMR** (Frimer et al., 1996; Afri et al., 2002, 2004a,b; Cohen et al., 2008a,b,c; Shachan-Tov et al., 2010), **Fluorescence** (Afri et al., 2011), and **ESR** (Bodner et al., 2010). These methods are based on the observation that in compounds bearing a polarizable moiety (e.g., carbonyl, nitronyl or phosphoryl groups) or a stable free radical, a good correlation exists between the solvent polarity in which the spectrum is obtained and the ^{13}C NMR chemical shift (δ) of the polarizable moiety, its fluorescence emission wavelength (λ_{em}), or a related ESR β-H splitting constants ($a_{\beta\text{-}H}$). In each of these cases, the polarity was assigned using the Dimroth–Reichardt $E_T(30)$ polarity parameter (Dimroth et al., 1963). The assumption in these cases is that the polarity within the bilayer is high at the water-lipid interface and drops as we approach the lipid slab.

Another well-known method for determining the depth of intercalants within liposomes is fluorescence quenching, which can be induced by a paramagnetic substances – often a stable nitroxide radical. These quenchers can be positioned at various points along a fatty acid chain. The basic assumption is that the closer the fluorophore lies to the quencher, the greater will be quenching. Once the positions of the nitroxides are independently determined, the depth of the matching fluorophore can be approximated as well. Thus, in the "**Parallax Method**" employed by London and others (Chattopadhyay and London, 1987; Abrams and London, 1993; London and Feigenson, 1981; Kachel et al., 1995; Bronshtein et al., 2004), the angstrom depth of an intercalant is determined by comparing the fluorescence quenching obtained with nitroxide quenchers at two different positions; the location of the intercalant is then calculated using the Perrin equation. We should note that the fluorescence systems are large and, hence, the exact "location" of the quenching is not really known. Authors generally assume quenching to occur at the center of the fluorescence emitting

* Corresponding author at: The Ethel and David Resnick Chair in Active Oxygen Chemistry, The Department of Chemistry, Bar-Ilan University, Ramat Gan, 5290002, Israel.

E-mail addresses: CAlexenber@nova.edu (C. Alexenberg), Michal.Afri@biu.ac.il (M. Afri), ShlomiEliyohu@gmail.com (S. Eliyahu), HaniPorat@gmail.com (H. Porat), Ayala.Ranz@gmail.com (A. Ranz), Aryeh.Frimer@biu.ac.il (A.A. Frimer).

https://doi.org/10.1016/j.chemphyslip.2019.03.018
Received 15 January 2019; Received in revised form 17 March 2019; Accepted 31 March 2019
Available online 04 April 2019
0009-3084/

fluorophore, but this is not at all clear – and, hence, the error in location could be quite large.

Fluorescence quenching can also be induced by molecules containing heavy atoms such as bromine or iodine. The literature is replete with examples, but for the most part the quenchers have either been vicinally substituted dibromophospholipids (Markello et al., 1985; Tennyson and Holloway, 1986; McIntosh and Holloway, 1987; Wiener and White, 1991), mixtures of homologous monobromophospholipids (Reinert et al., 1977) or phospholipids brominated at the terminal fatty acid carbon (Cudmore et al., 1994). Surprisingly, there seems to be little, if any, mention of the synthesis of the corresponding iodophospholipids or their use in fluorescence quenching. In any case, this quenching method, too, suffers from the drawback of not knowing the exact locus of quenching.

The above studies were carried out on liposomes, which are good models for biomembranes. In recent papers, Afri et al. (2014c) have implemented the aforementioned "NMR technique" for determining the location of intercalants within bilayers of biomembranes and erythrocyte ghosts. In addition, Afri et al. (2011) have shown that the intercalant location within bilayers can also be determined based on a correlation between a solvent's polarity and the fluorescence emission wavelength (λ_{em}) of the intercalant fluorophore. As before, it is assumed that the polarity within the bilayer is high at the water-lipid interface and very low as we approach the lipid slab. Both the NMR and fluorescence methods are complementary and allow us to expand our understanding of the depth penetration of fluorophore molecules within various lipid bilayer systems.

In this paper, we have intercalated nine compounds comprising five families of fluorophores **1–5** (see Fig. 1) into the lipid bilayer of three different lipid systems: (a) saturated lipid dimyristoylphosphatidylcholine (DMPC) liposomes; (b) bioliposomes prepared from a lipid mixture extracted from erythrocytes; and (c) erythrocyte ghosts. The families included three homologous protoporphyrins **1** (PP2, PP3 and PP7); three homologous hematoporphyrins **2** (HP2, HP7 and HP9); coumarin-314 (**3**); resorufin (7-hydroxy-3H-phenoxazin-3-one; **4**); and 4-chloro-7-nitrobenzofurazan (NBD, **5**). In the case of the porphyrins **1** and **2**, the digit in the name represents the number of methylenes in the fatty acid chain.

To serve as fluorescence quenchers, we have synthesized two series of halo-phospholipids. The first series included four new monobromophospholipids: 1-palmitoyl-2-(2-bromopalmitoyl)phosphatidylcholine (2-BrPPPC **14a)** and 1-palmitoyl-2-(*n*-bromostearoyl) phosphatidylcholine, where n = 6, 10 or 14 (6, 10 or 14-BrPSPC; **14b–d**], as outlined in Scheme 1. The second series was comprised of the corresponding four new monoiodophospholipids: 1-palmitoyl-2-(2-iodopalmitoyl)phosphatidylcholine (2-IPPPC; **17a**); and 1-palmitoyl-2-(*n*-iodostearoyl)phosphatidylcholine, where n = 6, 10 or 14 (6, 10 and 14-IPSPC; **17b–d**), as shown in Scheme 2.

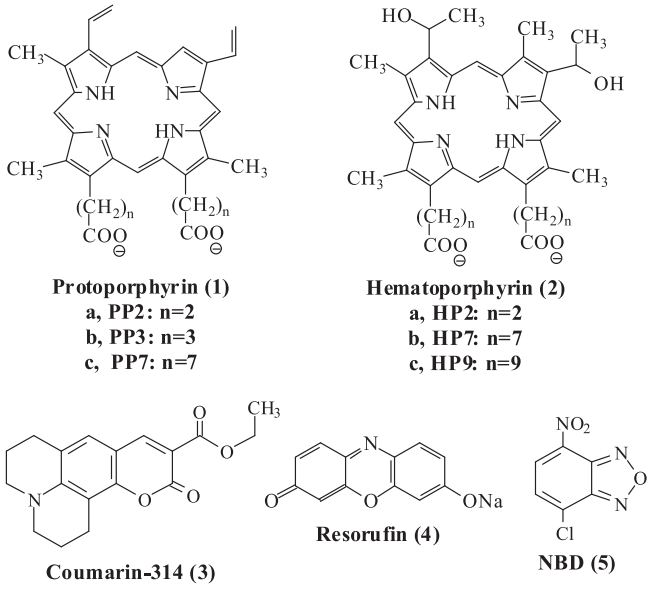

Fig. 1. Chemical structures of the fluorescent intercalants used in this study.

These new bromophosphatidylcholines (BrPCs) and iodophosphatidylcholines (IPCs) were mixed in turn with the lipid material of the various liposomal systems. Each of the fluorescent families **1–5** were then successively intercalated into the various liposomal matrices and the extent of fluorescence quenching was determined in each case. Our results are described below.

2. Materials and methods

2.1. General

Molecular modeling calculations were carried out with PCMODEL version 7.50.00, Serena Software, Bloomington, Indiana, USA – which uses the MMX force field. The **NMR** spectra were recorded on a Bruker DPX 300, DMX 600 or Avance III 700 Fourier transform spectrometer, while locked on the deuterium signal of the respective solvent at 25 ± 1 °C. The chemical shifts were measured relative to internal tetramethylsilane (TMS). The designation "t" indicates a triplet with second order coupling or broadening. ^{1}H and ^{13}C NMR spectra of bromophospholipids **14a–d** and iodophospholipids **17a–d** appear in the Supplemental materials section of this paper. **Fluorescence emission** spectra measurements were performed on a digital PC-controlled fluorimeter (Cary-Eclipse, Varian). Other standard equipment utilized included a vortex (Winn Vortex Genie) and a sonicator (Titanium Probe Vibra-Cell High Intensity Ultrasonic Liquid processors, model VCX-130, at a 20 KHz output frequency). **The numbering of the hydrogens and carbons** in halophospholipids **14** and **17** is exemplified below for 1-palmitoyl-2-(6″-bromostearoyl)-*sn*-glycero-3-phosphatidylcholine **(**6-BrPSPC**, 14b)**. We note that for 2-BrPPPC and for 2-IPPPC (compounds **14a** and **17a**), the fatty acid chain connected to glycerol carbon 2 is two carbons shorter (C_{16}) than analogs **b–d** (C_{18}), but we assume that this will have a negligible effect on the sample's location.

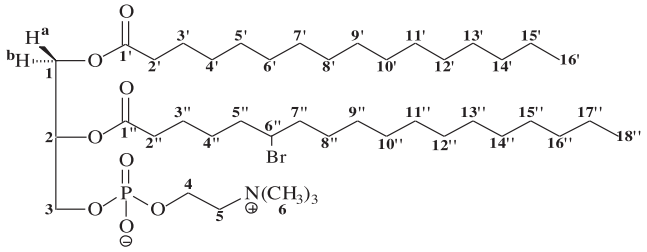

2.2. Chemicals

The protoporphyrins **1** and hematoporphyrins **2** were synthesized as previously described (Bronshtein et al., 2004) and dubbed PP2, PP3, PP7 and HP2, HP7, HP9, respectively. The digit in the abbreviations corresponds to the number of methylenes in each of the two side chains. Coumarin-314 (**3**, Sigma-Aldrich), Resorufin **4** (Molecular Probes), and 4-chloro-7-nitrobenzofurazan (NBD, **5** Sigma-Aldrich) were commercially available and used as supplied. Dimyristoylphosphatidylcholine (DMPC), 2-bromopalmitic acid (**12a**), *n,n*'-dicyclohexylcarbodiimide (DCC), 4-(dimethylamino)pyridine (DMAP), ethylenediaminetetraacetic acid (EDTA), 4-(2-hydroxyethyl)-1-piperazineethanesulfonic acid (HEPES), triphenylphosphine, iodine, NaI, KI and KBr were obtained from Sigma-Aldrich. Barium hydroxide octahydrate (Fluka), Tris-HCl (ACROS), sodium azide (Fisher Scientific), triphenylphospine

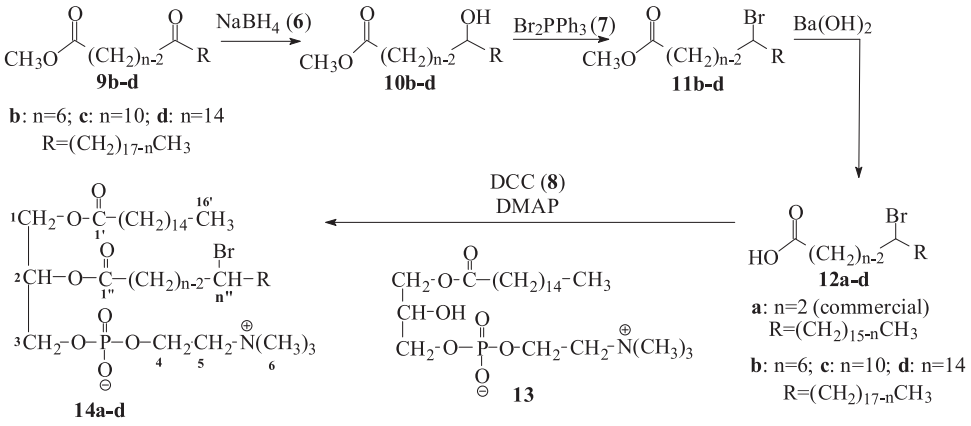

Scheme 1. Synthesis of *n*-bromophospholipids **14a–d**.

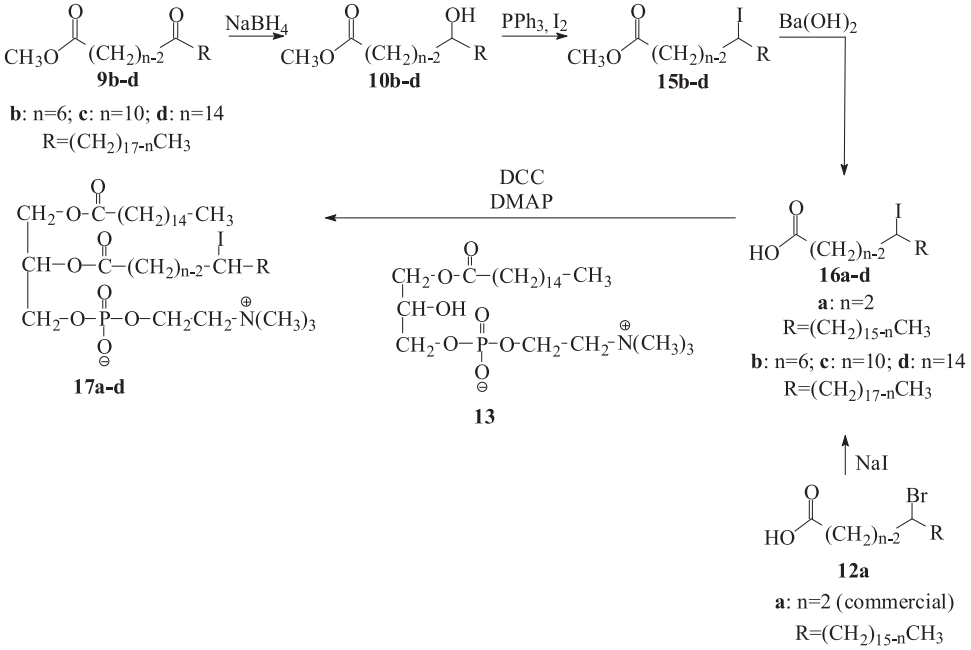

Scheme 2. Synthesis of *n*-iodophospholipids **17a–d**.

dibromide (Strem Chemicals) and 1-palmitoyl-2-hydroxy-*sn*-glycero-3-phosphatidylcholine (**13,** lyso 16:0) (Avanti Polar Lipid) were all commercially available. Fresh healthy human blood (units of ca. 0.5 L) was obtained from the blood bank of Chaim Sheba Medical Center at Tel-Hashomer Hospital, Ramat Gan, Israel.

Phosphate buffered saline solution pH 7.4 (PBS-N_3) was prepared using doubly distilled water (dd H_2O - purified via Millipore Milli-Q columns) containing 1.7 mM NaH_2PO_4, 8.1 mM Na_2HPO_4, 2.7 mM KCl, 137 mM NaCl and 0.1 wt% sodium azide. NaN_3 (0.1% or 1 g/L) is added as a preservative to prevent the formation of biological pathogens (Albrechtsen, 2006). **Ghost lysis medium** (pH = 7.2) was prepared from 250 mL dd H_2O, Tris-HCl (394 mg, 10 mM), EDTA (20.2 mg, 0.2 mM) and NaN_3 (0.25 g, 0.1%). **Ghost resealing medium** (pH = 7.4) was prepared from 250 mL of dd H_2O, KCl (2.796 g, 150 mM), HEPES (0.595 g, 10 mM), EDTA (0.051 g, 0.5 mM) and NaN_3 (0.25 g, 0.1%).

2.3. Synthesis of *n*-bromophospholipids *14a-d*

The synthesis of *n*-bromophospholipids **14a-d** begins with *n*-ketoesters **9b–d** or commercially available **12a**, as outlined in Scheme 1.

2.3.1. Preparation of *n*-hydroxystearate esters *10b–d*

n-Ketoesters **9b–d** were previously described by Afri et al. (2014a). $NaBH_4$ reduction of the latter, as described by Menger et al. (1989), yielded the corresponding hydroxyesters **10b–d**. The products in each case were conveniently identified by their spectral data. The ^{13}C NMR spectral data for **10b–d** have been previously reported by Tulloch (1978) – though our chemical shifts and assignments are more complete and somewhat different.

2.3.1.1. Methyl 6-hydroxyoctadecanoate (10b). 94% yield, mp 48 °C; ^1H NMR ($CDCl_3$) δ 3.69 (s, 3H, OCH_3), 3.62 (s, 1H, H_6), 2.35 (t, J = 7.2 Hz, 2H, H_2), 1.68 (m, 2H, H_3), 1.45 (m, 8H, H_4–H_5 and H_7–H_8), 1.28 (m, 18H, H_9–H_{17}, methylenes), 0.90 ("t", J = 7 Hz, 3H, H_{18}). ^{13}C NMR ($CDCl_3$) δ 174.73 (C_1), 71.75 (C_6), 51.79 (OCH_3), 37.36 and 37.00 (C_5 and C_7), 34.62 (C_2), 32.47 (C_{16}), 30.12, 29.66 and 29.37 (C_9–C_{15}, methylenes), 25.65, 25.46 and 25.21 (C_3, C_4 and C_8), 22.70 (C_{17}), 14.13 (C_{18}). MS (DCI, CH_4) m/z 297.282 (MH^+-H_2O, 100%); anal. HRMS (CI): calcd ($C_{19}H_{39}O_3$, MH^+) 297.2794 obsd. 297.2818. FTIR 3416 (vbr s, OH), 2926 (s), 2856 (m), 1747 (s, C═O), 1439 (w), 1199 (m, C–O) cm^{-1}.

2.3.1.2. Methyl 10-hydroxyoctadecanoate (10c). 96% yield, mp 47 °C;

^{1}H NMR ($CDCl_3$) δ 3.58 (s, 3H, OCH_3), 3.50 (bs, 1H, OH), 2.23 (t, J = 7.5 Hz, 2H, H_2), 1.54 (m, 2H, H_3), 1.35 (m, 8H, H_8, H_9, H_{11} and H_{12}), 1.28 (m, 18H, H_4–H_7 and H_{13}–H_{17}), 0.80 (t, J = 6.5 Hz, 3H, H_{18}). ^{13}C NMR ($CDCl_3$) δ 174.04 (C_1), 72.12 (C_{10}), 60.28 (OCH_3), 37.63 and 37.58 (C_9 and C_{11}), 34.05 (C_2), 32.01 (C_{16}), 29.85, 29.74, 29.53, 29.41, 29.32 and 29.23 (methylenes: C_4–C_7 and C_{13}–C_{15}), 25.78 and 25.74 (C_8 and C_{12}), 25.09 (C_3), 22.79 (C_{17}), 14.22 (C_{18}). MS (CI, CH_4) m/z 297.281 (MH^+-H_2O, 100%); anal. HRMS (CI): calcd ($C_{19}H_{39}O_3$, MH^+-H_2O) 297.279 obsd. 297.281. FTIR (KBr) 2916 and 2848 (s), 1732 (w, C═O), 1435 and 1381 (w), 1174 (w, C–O) cm^{-1}.

2.3.1.3. Methyl 14-hydroxyoctadecanoate (10d). 100% yield, mp 47 °C; ^{1}H NMR ($CDCl_3$) δ 3.60 (3H, s, OCH_3), 3.58 (1H, m, H_{14}), 2.29 (2H, t, J = 6.87 Hz, H_2) 1.61 (2H, m, H_3), 1.42 (4H, m, H_{13} and H_{15}), 1.25 (22H, m, methylenes: H_4–H_{12} and H_{16}–H_{17}), 0.90 (3H, "t", J = 6.4 Hz, H_{18}). ^{13}C NMR ($CDCl_3$) δ 174.52 (C_1), 72.17 (C_{14}), 51.58 (OCH_3), 37.62 and 37.3 (C_{13} and C_{15}), 34.26 (C_2), 29.85, 29.73, 29.57, 29.38 and 29.29 (methylenes: C_4–C_{11}), 27.98 (C_{16}), 25.79 and 25.1 (C_3 and C_{12}), 22.91 (C_{17}), 14.22 (C_{18}). MS (CI, CH_4) m/z 297.282 ($(M\text{-}OH)^+$, 16.97%), 265.242 ($(M\text{-}OH)^+$-MeOH, 20.92%); anal. HRMS (CI): calcd ($C_{19}H_{37}O_2$, $(M\text{-}OH)^+$) 297.2794 obsd. 297.2816. FTIR (KBr) 3412 (vbr s, OH), 2919, 2845 (?), 1744 (s, C═O) cm^{-1}.

*2.3.2. Preparation of bromostearate esters **11b–d***

Bromoesters **11b–d** were prepared from the corresponding hydroxyesters **10b–d** with triphenylphosphine dibromide according to the procedure of Balachander and Sukenik (1990), or via the method of Wiley et al. (1964) with the following modifications: (1) the reaction was carried out in dichloromethane (not DMF); (2) the product was purified by extraction into cold hexane to give the pure bromide esters as a yellow oil.

2.3.2.1. Methyl 6-bromostearate (11b). 98% yield; ^{1}H NMR ($CDCl_3$) δ 4.01 (quintet, J = 7.5 Hz, 1H, H_6), 3.67 (s, 3H, OCH_3), 2.34 (t, J = 7.5 Hz, 2H, H_2), 1.82 (m, 4H, H_5 and H_7), 1.26 (m, 24H, H_3–H_4 and H_8–H_{17}, methylenes), 0.88 ("t", J = 6.5 Hz, 3H, H_{18}). ^{13}C NMR ($CDCl_3$) δ 174.00 (C_1), 58.38 (C_6), 51.54 (OCH_3), 39.19 and 38.76 (C_5 and C_7), 33.90 (C_2), 29.70, 29.65, 29.58, 29.49, 29.36, 29.19 and 29.05 (C_9–C_{16}, methylenes), 27.58 and 27.14 (C_4 and C_8), 24.35 (C_3), 22.70 (C_{17}), 14.13 (C_{18}). MS (DCI, CH_4) m/z 379.209 (MH^+ + 2, 3.95%), 377.202 (MH^+ and M-H + 2, 9.32%,), 375.197, (M-H, 5.38%), 297.281 (MH^+-HBr, 100%); anal. HRMS (CI): calcd ($C_{19}H_{38}O_2{}^{79}Br$, MH^+) 377.2055 obsd. 377.2017. FTIR 2963 (s), 2940 (s), 2853 (m), 1753 (s, C═O), 1539 (w), 1474 (w), 1236 (m, C–O), 698 (w, C–Br) cm^{-1}.

2.3.2.2. Methyl 10-bromostearate (11c). 91% yield; ^{1}H NMR ($CDCl_3$) δ 3.98 (quintet, J = 7 Hz, 1H, H_{10}), 3.63 (s, 3H, OCH_3) 2.27 (t, J = 7.5 Hz, 2H, H_2), 1.77 (m, 4H, H_9 and H_{11}), 1.58 (m, 2H, H_3), 1.5 (m, 4H, H_8 and H_{12}), 1.27 (m, 18H, methylenes: H_4–H_7 and H_{13}–H_{17}), 0.85 ("t", J = 6.5 Hz, 3H, H_{18}). ^{13}C NMR ($CDCl_3$) δ 174.30 (C_1), 58.87 (C_{10}), 51.45 (OCH_3), 39.32 and 39.28 (C_9 and C_{11}), 34.49 (C_2), 31.98 (C_{16}), 29.58, 29.50, 29.40, 29.37, 29.29 and 29.21 (methylenes: C_4–C_7 and C_{13}–C_{15}), 27.71 and 27.67 (C_8 and C_{12}), 25.08 (C_3), 22.78 (C_{17}), 14.22 (C_{18}). MS (CI, CH4) m/z 379.213 (MH^+ + 2, 12.34%), 377.207 (MH^+ and M-H^+ + 2, 21.30%), 375.209 (MH^+, 5.85%), 297.248 (MH^+-HBr, 100%), 265.248 (MH^+-HBr-MeOH, 87.45%); anal. HRMS (CI): calcd ($C_{19}H_{38}O_2{}^{79}Br$, MH^+) 377.2055, obsd. 377.2067. FTIR 2927 and 2857 (s), 1742 (w, C═O), 1442 (w), 1179 (w, C–O), 721 (w, C–Br) cm^{-1}.

2.3.2.3. Methyl 14-bromostearate (11d). 83% yield; ^{1}H NMR ($CDCl_3$) δ 3.98 (quintet, J = 6 Hz, 1H, H_{14}), 3.62 (s, 3H, OCH_3) 2.26 (t, J = 4.5 Hz, 2H, H_2), 1.77 (m, 4H, H_{13} and H_{15}), 1.58 (m, 2H, H_3), 1.47 (m, 4H, H_{12} and H_{16}), 1.27 (m, 18H, methylenes: H_4–H_{11} and H_{17}), 0.9 ("t", J = 6.5 Hz, 3H, H_{18}). ^{13}C NMR ($CDCl_3$) δ 174.24 (C_1), 58.81 (C_{14}), 51.41 (OCH_3), 39.24 and 38.95 (C_{13} and C_{15}), 34.12 (C_2), 29.80 (C_{16}), 29.61, 29.54, 29.49, 29.31, 29.20 and 29.12 (methylenes: C_4–C_{11}), 27.63 (C_{12}), 25.00 (C_3), 22.23 (C_{17}), 14.01 (C_{18}). MS (CI, CH_4) m/z 379.207 (MH^+ + 2, 22.70%), 377.204 ($[MH]^+$, 25.09%), 297.286 (MH^+-HBr, 100%), 265.271 (MH^+-HBr-MeOH, 74.86%); anal. HRMS (CI): calcd. ($C_{19}H_{38}O_2{}^{79}Br$, MH^+) 377.2055, obsd. 377.2042. FTIR 2927 and 2857 (s), 1743 (w, C═O), 1456 (w), 1213 (w, C–O), 734 (w, C–Br) cm^{-1}.

*2.3.3. Preparation of n-bromostearic acids **12a–d***

2-Bromopalmitic acid (**12a**) is commercially available (Sigma-Aldrich). *n*-Bromoacids **12b–d** were obtained via the barium hydroxide octahydrate mediated saponification of bromoesters **11b–d**, respectively, following the procedure of Tanaka (1959).

2.3.3.1. 6-Bromostearic acid (12b). 60% yield, mp 47 °C; ^{1}H NMR ($CDCl_3$) δ 4.00 (quintet, J = 6.5 Hz, 1H, H_6), 2.38 (t, J = 7 Hz, 2H, H_2), 1.82 (m, 4H, H_5 and H_7), 1.63 (m, 4H, H_4 and H_8), 1.25 (m, 20H, H_3 and H_9-H_{17}, methylenes), 0.88 ("t", J = 6.5 Hz, 3H, H_{18}). ^{13}C NMR ($CDCl_3$) δ 178.73 (C_1), 58.23 (C_6), 39.22 and 38.75 (C_5 and C_7), 33.69 (C_2), 31.94 (C_{16}), 29.71, 29.68, 29.65, 29.58, 29.50, 29.36,29.06 (C_9–C_{15}, methylenes), 27.59 and 27.15 (C_4 and C_8), 24.10 (C_3), 22.70 (C_{17}), 14.13 (C_{18}). MS (DCI, CH_4) m/z 365.165 (MH^+ + 2, 2.39%), 363.192 (MH^+, 2.27%); 363.192 (MH^+, 2.27%, 3.95%); 283.258 (MH^+-HBr, 86.7%), 265.253 (MH^+-HBr-MeOH, 57.42%); anal. HRMS (CI): calcd ($C_{18}H_{36}O_2{}^{79}Br$, MH^+) 363.1899 obsd. 363.1924. FTIR 2915 (s), 2848 (s), 1693(s, C═O), 1464 (w), 1259 (m, C–O), 721 (w, C–Br) cm^{-1}.

2.3.3.2. 10-Bromostearic acid (12c). 88% yield, mp 45 °C; ^{1}H NMR ($CDCl_3$) δ 4.00 (quintet, J = 6 Hz, 1H, H_{10}), 2.32 (t, J = 7.5 Hz, 2H, H_2), 1.77 (m, 4H, H_9 and H_{11}), 1.61 (m, 2H, H_3), 1.52 (m, 4H, H_8 and H_{12}), 1.27 (m, 18H, methylenes: H_4–H_7 and H_{13}–H_{17}), 0.86 ("t", J = 7 Hz, 3H, H_{18}). ^{13}C NMR ($CDCl_3$) δ 180.357 (C_1), 58.9 (C_{10}), 39.27 and 39.22 (C_9 and C_{11}), 34.19 (C_3), 31.936 (C_{17}), 29.54, 29.45, 29.33, 29.22, 29.16 and 29.07 (methylenes: C_5–C_8 and C_{13}–C_{15}), 27.66 and 27.615 (C_8 and C_{12}), 24.72 (C_3), 22.74 (C_{17}), 14.18 (C_{18}). MS (CI, CH_4) m/z 283.264 (MH^+-HBr, 100%), 265.244 (MH^+-HBr-MeOH, 48.83%); anal. HRMS (CI): calcd ($C_{18}H_{36}O_2$, MH^+-HBr) 283.2637, obsd. 283.2643. FTIR 2912 and 2853 (s), 1693 (w, C═O), 1469 and 1418 (w), 1212 (w, C–O), 814 (w, C–Br) cm^{-1}.

2.3.3.3. 14-Bromostearic acid (12d). 80% yield, mp 45 °C; ^{1}H NMR ($CDCl_3$) δ 4.02 (quintet, J = 6 Hz, 1H, H_{14}), 2.33 (t, J = 7.5 Hz, 2H, H_2), 1.8 (m, 4H, H_{13} and H_{15}), 1.62 (m, 2H, H_3), 1.44 (m, 4H, H_{12} and H_{16}), 1.26 (m, 18H, methylenes: H_4–H_{11} and H_{17}), 0.86 ("t", J = 6.5 Hz, 3H, H_{18}). ^{13}C NMR ($CDCl_3$) δ 180.33 (C_1), 59.06 (C_{14}), 39.30 and 39.00 (C_{13} and C_{15}), 34.22 (C_2), 29.85 (C_{16}), 29.85, 29.65, 29.60, 29.53, 29.35 and 29.17 (methylenes: C_4–C_{11}), 27.69 (C_{12}), 24.79 (C_3), 22.29 (C_{17}), 14.09 (C_{18}). MS (CI, CH_4) m/z 283.261 (MH^+-HBr, 99.98%), 265.256 (MH^+-HBr-MeOH, 64.08%); anal. HRMS (CI): calcd ($C_{18}H_{36}O_2$, MH^+-HBr) 283.2637, obsd. 283.2612. FTIR 2913 and 2851 (s), 1695 (w, C═O), 1469 and 1421 (w), 1209 (w, C–O), 816 (w, C–Br) cm^{-1}.

*2.3.4. Preparation of bromophospholipids **14a–d***

Following the procedure of Menger et al. (1989), bromoacids **12a–d** (3.5 equiv.), 1-palmitoyl-2-hydroxy-*sn*-glycero-3-phosphatidylcholine (**13**, 1 equiv.), DMAP (2 equiv.) and DCC (2.5 equiv.) were dried under vacuum, dissolved in dry chloroform, and injected in the order mentioned above into a two necked round bottom reaction flask under nitrogen. The solution was stirred at room temperature from 4 h to 48 h, depending on the derivative (4 h for derivative **14a**, 30 h for derivatives **14b** and **14d**, and 48 h for derivative **14c**). The solvent was evaporated and the residue was purified by flash chromatography, eluting with mixtures ranging from 20:80 to 50:50 methanol:chloroform. The products were obtained as white solids and identified by their spectral

data. The NMR reveals varying amounts of lysoPC **13**.

2.3.4.1. 1-Palmitoyl-2-(2′′-bromopalmitoyl)-sn-glycero-3-phosphatidylcholine (14a). 74% yield, Phase Transition Temp. (melt): 172–174 °C; ^{1}H NMR ($CDCl_3$) δ 5.28 (m, 1H, H_2), 4.40 (m, 1H, H_{1b}), 4.27 (m, 2H, H_4), 4.21 (m, 1H, H_{1a}), 4.08 (m, 1H, $H_{2''}$), 3.99 (m, 2H, H_3), 3.86 (m, 2H, H_5), 3.37 (s, 9H, H_6), 2.26 (m, 2H, $H_{2'}$), 1.96 (m, 2H, $H_{3''}$), 1.58 (m, 2H, $H_{3'}$), 1.29 (m, 48H, methylenes: $H_{4'}$–$H_{15'}$ and $H_{4''}$–$H_{15''}$), 0.88 (”t”, J = 7 Hz, 6H, $H_{16'}$ and $H_{16''}$). ^{13}C NMR ($CDCl_3$) δ 173.85 and 169.54 ($C_{1'}$ and $C_{1''}$), 72.18 (d, Jcp = 7.5 Hz, C_4), 66.89 (d, Jcp = 6.5 Hz, C_5), 63.76 (d, Jcp = 3 Hz, C_2), 62.46 (C_1), 59.83 (d, Jcp = 3 Hz, C_3), 54.56 (C_6), 45.80 ($C_{2''}$), 34.96 ($C_{2'}$ and $C_{3''}$), 31.93 ($C_{14'}$ and $C_{14''}$), 29.73, 29.68, 29.63, 29.57, 29.46, 29.37, 29.29, 29.23, 28.97 and 28.81 (methylenes: C_4–$C_{13'}$ and $C_{5''}$–$C_{13''}$), 27.26 ($C_{4''}$), 24.87 ($C_{3'}$), 22.68 ($C_{15'}$ and $C_{15''}$), 14.09 ($C_{16'}$ and $C_{16''}$). MS (TOF-ES+) *m/z*: 814.48 (MH^+ + 2, 99.1%), 812.48 (MH^+ 100%), 496.32 (MH^+-CO-$C_{15}H_{30}Br$, 71.9%). HRMS (MALDI matrix THAP) *m/z* calc. ($C_{40}H_{80}{}^{79}BrNO_8P$, MH^+) 812.4740, obsd. 812.4799. FTIR 2916 and 2850 (s), 1733 (m, C═O) 1473 (m), 1240 (m, C−O and P═O), 1062 (s), 865 (w, P−O−R-ester), 814 (w, C−Br) cm^{-1}.

2.3.4.2. 1-Palmitoyl-2-(6′′-bromostearoyl)-sn-glycero-3-phosphatidylcholine (14b). 71% yield. Phase Transition Temp (melt): 167–169 °C; ^{1}H NMR ($CDCl_3$) δ 5.20 (m, 1H, H_2), 4.39 (m, 1H, H_{1b}), 4.30 (m, 2H, H_4), 4.11 (m, 1H, H_{1a}), 4.00 (m, 1H, $H_{6''}$), 3.94 (m, 2H, H_3), 3.75 (m, 2H, H_5), 3.32 (s, 9H, H_6), 2.39 (m, 6H, $H_{2'}$,$H_{2''}$ and $H_{5''}$), 1.80 (m, 10H, $H_{3'}$, $H_{3''}$, $H_{4''}$, $H_{7''}$ and $H_{8''}$), 1.57 (m, 8H, $H_{4'}$, $H_{5'}$, $H_{9''}$ and $H_{10''}$), 1.26 (m, 34H, methylenes: H_6–$H_{15'}$ and $H_{11''}$–$H_{17''}$), 0.88 (”t”, J = 7 Hz, 6H, $H_{16'}$ and $H_{18''}$). ^{13}C NMR ($CDCl_3$) δ 173.66 and 172.97 ($C_{1'}$ and $C_{1''}$), 70.63 (d, Jcp = 7 Hz, C_4), 66.43 (d, Jcp = 5.5 Hz, C_5), 63.51 (d, Jcp = 4 Hz, C_2), 62.59 (C_1), 59.36 (d, Jcp = 4 Hz, C_3), 58.59 ($C_{6''}$), 54.49 (C_6), 39.38 and 38.87 ($C_{5''}$ and $C_{7''}$), 34.17 and 34.13 ($C_{2'}$ and $C_{2''}$), 31.95 ($C_{14'}$ and $C_{16''}$), 30.94, 29.77, 29.71, 29.66, 29.63, 29.59, 29.40, 29.25, 29.16 and 29.06 (methylenes: C4′-C13′ and C9′′–C15′′), 27.70 and 27.21 (C4′′ and C8′′), 24.93 and 24.35 ($C_{3'}$ and $C_{3''}$), 22.71 ($C_{15'}$ and $C_{17''}$), 14.14 ($C_{16'}$ and $C_{18''}$). MS (TOF-ES+) *m/z*: 842.51 (MH^+ + 2, 100%), 840.51 (MH^+ 89.5%), 496.32 (MH^+ − CO-$C_{17}H_{34}Br$, 81.6%). HRMS (MALDI matrix DHB) *m/z* calc. ($C_{42}H_{84}{}^{79}BrNO_8P$,$MH^+$) 840.5112, obsd. 840.5050. FTIR 2920 (s), 2852 (s), 1737 (m, C═O) 1477 (m), 1237 (m, C−O and P═O) and 1062 (s), 866 (w, P-O-R-ester) 816 (w, C−Br) cm^{-1}.

2.3.4.3. 1-Palmitoyl-2-(10′′-bromostearoyl)-sn-glycero-3-phosphatidylcholine (14c). 46% yield, Phase Transition Temp (melt): 177–179 °C; ^{1}H NMR ($CDCl_3$) δ 5.19 (m, 1H, H_2), 4.40 (m, 1H, H_{1b}), 4.38 (m, 2H, H_4), 4.10 (m, 1H, H_{1a}), 4.01 (m, 1H, $H_{10''}$), 3.92 (m, 2H, H_3), 3.77 (m, 2H, H_5), 3.33 (s, 9H, H_6), 2.27 (2″t”, J = 7.5 Hz, 4H, $H_{2'}$ and $H_{2''}$), 1.79 (m, 4H, $H_{9''}$ and $H_{11''}$), 1.57 (m, 8H, $H_{3'}$, $H_{3''}$, $H_{8''}$ and $H_{12''}$), 1.26 (m, 42H, methylenes: H_4–$H_{15'}$, $H_{4''}$–$H_{7''}$ and $H_{13''}$–$H_{17''}$), 0.88 (2″t”, J = 6, 6H, $H_{16'}$ and $H_{18''}$). ^{13}C NMR ($CDCl_3$) δ 173.63 and 173.27 ($C_{1'}$ and $C_{1''}$), 70.54 (d, Jcp = 4 Hz, C_4), 66.47 (d, Jcp = 5.5 Hz, C_5), 63.58 (d, Jcp = 4.5 Hz, C_2), 63.03 (C_1), 59.39 (d, Jcp = 4 Hz, C_3), 58.95 ($C_{10''}$), 54.504 (C_6), 39.29 and 39.26 ($C_{9''}$ and $C_{11''}$), 34.33 and 34.18 ($C_{2'}$ and $C_{2''}$), 31.96 and 31.88 ($C_{14'}$ and $C_{16''}$), 29.77, 29.71, 29.63, 29.49, 29.45, 29.40, 29.34, 29.27, 29.22 and 29.13 (methylenes: C_4–$C_{13'}$, $C_{4''}$–$C_{7''}$ and $C_{13''}$–$C_{15''}$), 27.65 ($C_{8''}$ and $C_{12''}$), 24.98 and 24.94 ($C_{3'}$ and $C_{3''}$), 22.71 and 22.68 ($C_{15'}$ and $C_{17''}$), 14.13 and 14.11 ($C_{16'}$ and $C_{18''}$). MS (TOF-ES+) *m/z*: 842.52 (MH^+ + 2, 94.4%), 840.51 (MH^+, 100%), 496.35 (MH^+-CO-$C_{17}H_{34}Br$, 78.9%). HRMS (MALDI matrix DHB) *m/z* calc. ($C_{42}H_{84}{}^{79}BrNO_8P$, MH^+) 840.5112, obsd. 840.5110. FTIR 2927 and 2859 (s), 1748 and 1725 (w, C═O), 1548 and 1486 (w), 1236 (w, C−O, P═O), 1086 (s), 864 (w, P−O−R), 813 (w, C−Br) cm^{-1}.

2.3.4.4. 1-Palmitoyl-2-(14′′-bromostearoyl)-sn-glycero-3-phosphatidylcholine (14d). 80% yield. Phase Transition Temp (melt): 186–188 °C; ^{1}H NMR ($CDCl_3$) δ 5.21 (m, 1H, H_2), 4.37 (m, 1H, H_{1b}), 4.28 (m, 2H, H_4), 4.13 (m, 1H, H_{1a}), 4.00 (m, 2H, $H_{14''}$), 3.89 (m. 2H, H_3), 3.79 (m, 2H, H_5), 3.38 (s, 9H, H_6), 2.29 (2 ”t”, J = 7 Hz, 4H, $H_{2'}$ and $H_{2''}$), 1.81 (m, 4H, $H_{13''}$ and $H_{15''}$), 1.58 (m, 8H, $H_{3'}$, $H_{3''}$ and $H_{12''}$), 1.26 (m, 44H, methylenes: $H_{4'}$–$H_{15'}$, $H_{4''}$–$H_{11''}$ and $H_{16''}$–$H_{17''}$), 0.88 (2 ”t”, J = 7, 6H, $H_{16'}$ and $H_{18''}$). ^{13}C NMR ($CDCl_3$) δ 173.57 and 173.21 ($C_{1'}$ and $C_{1''}$), 70.29 (d, Jcp = 6.5 Hz, C_4), 66.41 (d, Jcp = 3 Hz, C_5), 63.90 (d, Jcp = 3 Hz, C_2), 62.80 (C_1), 59.72 (C_3), 58.94 ($C_{14''}$), 54.61 (C_6), 39.23 and 39.93 ($C_{13''}$ and $C_{15''}$), 34.34 and 34.16 ($C_{2'}$ and $C_{2''}$), 31.95 ($C_{14'}$), 29.74, 29.69, 29.64, 29.58, 29.56, 29.39, 29.22, 29.19 and 29.13 (methylenes: C_4–$C_{13'}$ and $C_{4''}$–$C_{11''}$), 27.63 ($C_{12''}$ and $C_{16''}$), 24.99 and 24.93 ($C_{3'}$ and $C_{3''}$), 22.71 and 22.20 ($C_{15'}$ and $C_{17''}$), 14.124 and 13.971 ($C_{16'}$ and $C_{18''}$). MS (TOF-ES+) m/z: 842.52 (MH^+ + 2, 97.6%), 840.51 (MH^+, 100%). HRMS (MALDI matrix DHB) m/z calc. ($C_{42}H_{84}{}^{79}BrNO_8P$, MH^+) 840.5112, obsd. 840.5110. FTIR 2921 and 2854 (s), 1748 (w, C═O), 1648 (s), 1548 and 1479 (w), 1237 (w, C−O,P═O), 1086 (s), 864 (w, P−O−R), 813 (w, C−Br) cm^{-1}.

2.4. Synthesis of n-iodophospholipids *17a–d:*

The synthesis of *n*-iodophospholipids **17a–d** begins, along the same lines as for the corresponding bromophospholipids, from *n*-ketoesters **9b–d** (through *n*-hydroxystearate esters **10b–d**) or commercially available **12a**, as outlined in Scheme 2.

2.4.1. Preparation of iodostearate esters *15b–d*

Iodooesters **15b–d** were prepared from the corresponding hydroxyesters **10b–d** with triphenylphospine and iodine according to the procedure of Meiresonne et al. (2012) with the following modifications: (1) the reaction was carried out under dryness conditions; (2) the reaction was carried out in dry chloroform (not dichloromethane); (3) The iodine was added in ice water bath to the flask with the hydroxystearate (1 equivalent.) and imidazole (2.3 equivalents), in several portions during a course of 2 h.; (4) the reaction was run at r.t. overnight; (5) the reaction was quenched by saturated sodium thiosulfate, distilled water and ether, dried, and purified by extraction into cold hexane – to give the pure iodide esters as a yellow oil.

2.4.1.1. Methyl 6-iodostearate (15b). 46% yield; ^{1}H NMR ($CDCl_3$) δ 4.01 (septet, J = 4 Hz, 1H, H_6), 3.57 (s, 3H, OCH_3), 2.25 (t, J = 7.5, 2 H Hz, H_2), 1.78 (m, 2H, H_5), 1.66–1.29 (m, 8H, H_3–H_4 and H_7–H_8), 1.19 (m, 18H, H_9- H_{17}, methylenes), 0.81 (”t”, J = 7 Hz, 3H, H_{18}). ^{13}C NMR (CDCl3): δ 172.63 (C_1), 50.41 (OCH_3), 39.71 and 39.27 (C_5 and C_7), 38.37 (C_6), 32.83 (C_2), 30.97 (C_{16}), 28.76, 28.72, 28.70, 28.64, 28.56, 28.54 and 28.41 (methylenes: C_9-C_{15}), 28.10 and 27.90 (C_4 and C_8), 23.15 (C_3), 21.73 (C_{17}), 13.16 (C_{18}). MS (TOF-ES+) *m/z*: 447 (MNa^+, 100%), 319 (MNa^+-HI, 27.52%), 279 (MNa^+-$C_{12}H_{24}$, 41.12%); anal. HRMS (ESI): calcd ($C_{19}H_{37}O_2I$, M^+) 424.182, obsd. 424.184. FTIR 2921 (s), 2852 (s), 1739 (s, C═O), 1436 (m), 1169 (s, C−O), 721 (m, C−I) cm^{-1}.

2.4.1.2. Methyl 10-iodostearate (15c). 46% yield; ^{1}H NMR ($CDCl_3$) δ 4.11 (septet, J = 4 Hz, 1H, H_{10}), 3.67 (s, 3H, OCH_3), 2.30 (t, J = 7.5 Hz, 2H, H_2), 1.85 (m, 2H, H_9), 1.68 (m, 2H, H_{11}), 1.62 (m, 2H, H_3), 1.52 (m, 2H, H_8), 1.39 (m, 2H, H_{12}), 1.30 (m, 18H, methylenes: H_4–H_7 and H_{13}–H_{17}), 0.88 (”t”, J = 7 Hz, 3H, H_{18}). ^{13}C NMR ($CDCl_3$): δ 174.29 (C_1), 51.45 (OCH_3), 40.70 and 40.68 (C_9 and C_{11}), 40.64 (C_{10}), 34.10 (C_2), 31.86 (C_{16}), 29.54, 29.50, 29.45, 29.32, 29.26, 29.17 and 29.10 (methylenes: C_4–C_7 and C_{13}–C_{15}), 28.87 and 28.78 (C_8 and C_{12}), 24.93 (C_3), 22.665 (C_{17}), 14.11 (C_{18}). MS (TOF-ES+) *m/z*: 447 (MNa^+, 100%), 335 (MNa^+-C_8H_{17} + H^+, 3.65%), 319 (MNa^+-HI, 11.1%); anal. HRMS (ESI): calcd ($C_{19}H_{37}O_2I$, M^+) 424.182, obsd. 424.184. FTIR 2923 and 2853 (s), 1739 (s, C═O), 1435 (m), 1169 (m, C−O), 720 (m, C−I) cm^{-1}.

2.4.1.3. Methyl 14-iodostearate (15d). 65% yield; ^{1}H NMR ($CDCl_3$)

δ 4.10 (septet, J = 4 Hz, 1H, H_{14}), 3.64 (s, 3H, OCH_3) 2.28 (t, J = 7.5 Hz, 2H, H_2), 1.82 (m, 2H, H_{13}), 1.68 (m, 2H, H_{15}), 1.60 ("quintet", J = 7.5 Hz, 2H, H_3), 1.49 (m, 2H, H_{12}), 1.36 (m, 2H, H_{16}), 1.25 (m, 18H, methylenes: H_4–H_{11} and H_{17}), 0.90 ("t", J = 7 Hz, 3H, H_{18}). ^{13}C NMR ($CDCl_3$): δ 174.21 (C_1), 51.35 (OCH_3), 40.62 and 40.54 (C_{13} and C_{15}), 40.34 (C_{14}), 34.33 (C_2), 31.63 (C_{16}), 29.51, 29.49, 29.47, 29.41, 29.37, 29.30, 29.19 and 29.09 (methylenes: C_4-C_{11}), 28.79 (C_{12}), 24.90 (C_3), 22.92 (C_{17}), 13.92 (C_{18}). MS (TOF-ES+) m/z: 447 (MNa^+, 100%), 399 (MNa^+-$C_4H_9+H^+$, 1.82%), 319 (MNa^+-HI, 22.43%); anal. HRMS (ESI): calcd ($C_{19}H_{37}O_2I$, M^+) 424.183, obsd. 424.184. FTIR 2923 and 2852 (s), 1739 (s, C═O), 1435 (m), 1169 (s, C−O), 721 (m, C−I) cm^{-1}.

2.4.2. Preparation of n-iodostearic acids **16a–d**

2.4.2.1. Preparation of 2-Iodopalmitic acid ***16a***. 2-Iodopalmitic acid (**16a**) was prepared from the commercially available 2-bromopalmitic acid (**12a**), with sodium iodide following the procedure of Ervithayasuporn et al. (2013)- with the following modifications: (1) the reaction was carried out under dry conditions; (2) the solvent used was dry acetonitrile (not acetone or THF); (3) the equivalent ratio bromostearic:NaI was 1:6.7; (4) the reaction was performed at r.t. for 2 days (not reflux for 3 days); (5) the product was extracted with ether and water, dried, recrystallized from hexane and purified 3 times on PLC Silica gel 60 F_{254} 2 mm, eluting with 100% ether - giving the pure acid as a white solid.

2.4.2.1.1. 2-Iodopalmitic acid (16a). 1.5% yield, mp 54 °C; ^{1}H NMR ($CDCl_3$) δ 4.31 (t, J = 7.5 Hz, 1H, H_2), 1.98 (m, 2H, H_3), 1.40 (m, 2H, H_4), 1.26 (m, 22H, H_5–H_{15}, methylenes), 0.88 ("t", 3H, J = 7 Hz, H_{16}). ^{13}C NMR ($CDCl_3$): δ 177.29 (C_1), 45.55 (C_2), 35.75 (C_3), 31.87 (C_{14}), 29.63, 29.61, 29.59, 29.59, 29.53, 29.42, 29.30, 29.26 and 29.24 (C_5–C_{13}, methylenes), 28.64 (C_5), 22.81 (C_6), 14.06 (C_{16}). MS (TOF-ES$^+$) m/z: 413 ($M^+ + CH_3OH$-H^+ 69.17%), 279 (MNa^+-HI, 100%), 224 (MK^+-$C_{14}H_{29}$, 1.94%); anal. HRMS (CI): calcd ($C_{16}H_{31}IO_2$, MH^-) 381.130, obsd. 381.130. FTIR: 2915 and 2848 (s), 1683 (s, C═O), 1463 (w), 1415 (m), 1232 (m, C−O), 858 (m, C−I) cm^{-1}.

2.4.2.2. Preparation of n-iodostearic acids ***16b–d***. *n*-Iodoacids **16b–d** were obtained via the barium hydroxide octahydrate mediated saponification of iodoesters **15b–d**, respectively, following the procedure of Tanaka (1959).

2.4.2.2.1. 6-Iodostearic acid (15b). 52% yield, mp 44 °C; ^{1}H NMR ($CDCl_3$) δ 4.10 (septet, J = 4 Hz, 1H, H_6), 2.38 (t, J = 7.5 Hz, 2H, H_2), 1.87 (m, 2H, H_5), 1.68 (m, 6H, H_3-H_4 and H_7), 1.35–1.55 (m, 4H, H_8 and H_9), 1.26 (m, 16H, H_{10}- H_{17}, methylenes), 0.88 ("t", J = 7 Hz, 3H, H_{18}). ^{13}C NMR ($CDCl_3$) δ 179.83 (C_1), 40.67 and 40.18 (C_5 and C_7), 39.57 (C_6), 33.86 (C_2), 31.90 (C_{16}), 29.68, 29.64, 29.62, 29.56, 29.50, 29.46, 29.33 (C_9-C_{15} methylenes), 28.00 and 28.82 (C_4 and C_8), 23.83 (C_3), 22.67 (C_{17}), 14.10 (C_{18}). MS (TOF-ES+) m/z: 433 (MNa^+, 100%), 305 (MNa^+-HI, 77%), 265 (MNa^+-$C_{12}H_{25}+H^+$, 60.42%); anal. HRMS (ESI): calcd ($C_{18}H_{35}O_2I$, M^+) 410.168, obsd. 410.168. FTIR : 2914 (s), 2847 (s), 1691 (m, C═O), 1470 (m), 1192 (w, C−O), 901 (w, C−I) cm^{-1}.

2.4.2.2.2. 10-Iodostearic acid (15c). 60% yield; ^{1}H NMR ($CDCl_3$) δ 4.11 (septet, J = 4 Hz, 1H, H_{10}), 2.35 (t, J = 7.5 Hz, 2H, H_2), 1.85 (m, 2H, H_9), 1.63 (m, 4H, H_3 and H_{11}), 1.52 (m, 2H, H_8), 1.30 (m, 20H, methylenes: H_4–H_7 and H_{12}–H_{17}), 0.89 ("t", J = 7 Hz, 3H, H_{18}). ^{13}C NMR ($CDCl_3$) δ 180.20 (C_1), 40.65 and 40.59 (C_9 and C_{11}), 40.55 (C_{10}), 34.04 (C_2), 31.81 (C_{16}), 29.49, 29.45, 29.41, 29.27, 29.205, 29.11 and 28.96 (methylenes: C_4–C_7 and C_{13}–C_{15}), 28.83 and 28.73 (C_8 and C_{12}), 24.60 (C_3), 22.62 (C_{17}), 14.07 (C_{18}). MS (TOF-ES+) m/z: 432 (MNa^+-H^+, 23.55%), 321 (MNa^+-$C_8H_{17}+H^+$, 100%), 305 (MNa^+-HI, 20.97%); anal HRMS (ESI): calcd ($C_{18}H_{35}O_2I$, M^+) 410.168, obsd. 410.168. FTIR 2922 and 2852 (s), 1707 (s, C═O), 1457 (m), 1281 (w, C−O), 722 (w, C−I) cm^{-1}.

2.4.2.2.3. 14-Iodostearic acid (15d). 67% yield; ^{1}H NMR ($CDCl_3$) δ 4.11 (septet, J = 4 Hz, 1H, H_{14}), 2.34 (t, J = 7.5 Hz, 2H, H_2), 1.84 (m, 2H, H_{13}), 1.68 (m, 2H, H_{15}), 1.63 ("quintet", J = 7.5 Hz, 2H, H_3), 1.50 (m, 2H, H_{12}), 1.26 (m, 20H, methylenes: H_4–H_{11} and H_{16}–H_{17}), 0.91 ("t", J = 7 Hz, 3H, H_{18}). ^{13}C NMR ($CDCl_3$) δ 180.18 (C_1), 40.65 (C_{13} or C_{15}), 40.61 (C_{14}), 40.36 (C_{13} or C_{15}), 34.06 (C_2), 31.66 (C_{16}), 29.52, 29.50, 29.44, 29.38, 29.20, 29.14, 29.03 and 28.98 (methylenes: C_4–C_{11}), 28.83 (C_{12}), 24.64 (C_3), 21.95 (C_{17}), 13.95 (C_{18}). MS (TOF-ES+) m/z: 410 (M^+, 16.38%), 393 (MK^+-$C_4H_9+H^+$, 14.07%), 321 (MK^+-HI, 100%); anal. HRMS (ESI): calcd ($C_{18}H_{35}O_2I$, M^+) 410.169, obsd. 410.168. FTIR 2922 and 2852 (s), 1707 (s, C═O), 1464 (m), 1229 (w, C−O), 731 (w, C−I) cm^{-1}.

2.4.3. Preparation of iodophospholipids **17a–d**

We followed the procedure of Menger et al. (1989) as described for bromophospholipids **14a–d**. Iodoacids **16a–d** (2.5 equiv.), 1-palmitoyl-2-hydroxy-*sn*-glycero-3-phosphatidylcholine (**13**, 1 equiv.), DMAP (2 equiv.) and DCC (2.5 equiv.) were dried under vacuum, dissolved in dry chloroform, and injected in the order mentioned above into a two necked round bottom reaction flask under nitrogen. The solution was stirred at room temperature from 4 to 26 h, depending on the derivative (4 h for derivative **17a**, 23 h for derivatives **17c** and **17d**, and 26 h for derivative **14b**). The solvent was evaporated and the residue was purified by flash chromatography, eluting with mixtures ranging from 20:80 to 50:50 methanol:chloroform. The products, obtained as a solid in the case of **17a** and as yellowish oils in the cases of **17b–d**, were identified by their spectral data.

2.4.3.1. 1-Palmitoyl-2-(2′′-iodopalmitoyl)-sn-glycero-3-phosphatidylcholine (17a). 34.5% yield, Decomp. temp.: 182–184 ºC; ^{1}H NMR ($CDCl_3$) δ 5.25 (m, 1H, H_2), 4.31 (m, 3H, H_{1b} and H_4), 4.07 (m, 2H, H_{1a} and $H_{2''}$), 3.96 (m, 2H, H_3), 3.59 (m, 2H, H_5), 3.37 (s, 9H, H_6), 2.30 (m, 2H, $H_{2'}$), 1.97 (m, 2H, $H_{3''}$), 1.58 (m, 2H, $H_{4''}$), 1.40 and 1.26 (m, 48H, methylenes: H_3–$H_{15'}$ and $H_{5''}$–$H_{15''}$), 0.88 ("t", J = 7 Hz, 6H, $H_{16'}$ and $H_{16''}$). ^{13}C NMR ($CDCl_3$): δ 173.60 and 173.49 ($C_{1'}$ and $C_{1''}$), 72.10 and 71.93 (d, Jcp = 7.5 Hz, C_4), 66.25 (d, Jcp = 4.5 Hz, C_5), 63.22 (d, Jcp = 3.5 Hz, C_2), 62.85 (C_1), 59.49, 54.57 (C_6), 36.17 ($C_{3''}$), 34.24 ($C_{2'}$), 31.96 ($C_{14'}$ and $C_{14''}$), 29.76, 29.67, 29.63, 29.48, 29.45, 29.37, 29.29, 29.25 and 28.86 (methylenes: C_4–$C_{13'}$ and $C_{5''}$–$C_{13''}$), 28.66 ($C_{4''}$), 24.99 ($C_{3'}$), 22.71 ($C_{15'}$ and $C_{15''}$), 21.65 ($C_{2''}$), 14.12 ($C_{16'}$ and $C_{16''}$). MS (TOF-ES+) m/z: 861.47 (MH^+, 91.6%), 496.34 (MH_2^+-CO-$C_{15}H_{30}I$, 100%). HRMS (MALDI matrix DHB) m/z: calcd ($C_{40}H_{79}INO_8P$, MH^+) 860.466, obsd. 860.466. FTIR 2917 and 2849 (s), 1733 (m, C═O) 1467 (m), 1241 (s, C−O and P═O), 1083 (s), 969 (w, P−O−R-ester), 802 (w, C−I) cm^{-1}.

2.4.3.2. 1-Palmitoyl-2-(6′′-iodostearoyl)-sn-glycero-3-phosphatidylcholine (17b). 58% yield; ^{1}H NMR ($CDCl_3$): δ 5.19 (m, 1H, H_2), 4.39 (m, 1H, H_{1b}), 4.30 (m, 2H, H_4), 4.08 (m, 2H, H_{1a}), 3.94 (m, 2H, $H_{6''}$), 3.80 (m, 2H, H_3), 3.66 (m, 1H, H_5), 3.361 (s, 9H, H_6), 3.157 (m, 4H, $H_{2'}$ and $H_{2''}$), 2.28 (m, 4H, $H_{5''}$ and $H_{7''}$), 1.84 (m, 2H, $H_{4''}$), 1.57 (m, 8H, $H_{3'}$-$H_{4'}$, $H_{3''}$ and $H_{8''}$), 1.25 (m, 40H, methylenes: $H_{5'}$- $H_{15'}$ and $H_{9''}$-$H_{17''}$), 0.88 ("t", 6H, J = 7 Hz, $H_{16'}$ and $H_{18''}$). ^{13}C NMR ($CDCl_3$): δ 173.57 and 172.85 ($C_{1'}$ and $C_{1''}$), 70.68 (d, Jcp = 7 Hz, C_4), 66.43 (d, Jcp = 5.50 Hz, C_5), 63.41 (d, Jcp = 4.5 Hz, C_2), 62.95 (C_1), 59.30 (d, Jcp = 5 Hz, C_3), 54.50 (C_6), 40.81 and 40.30 ($C_{5''}$ and $C_{7''}$), 40.08 ($C_{6''}$), 34.16 and 34.11 ($C_{2'}$ and $C_{2''}$), 31.92 ($C_{14'}$ and $C_{16''}$), 29.72, 29.67, 29.65, 29.62, 29.57, 29.53, 29.37, 29.21, 29.15 and 29.91 (methylenes: C_4–$C_{13'}$ and $C_{9''}$–$C_{15''}$), 28.91 and 28.83 ($C_{4''}$ and $C_{8''}$), 24.91 and 24.13 ($C_{3'}$ and $C_{3''}$), 22.68 ($C_{15'}$ and $C_{17''}$), 14.11 ($C_{16'}$ and $C_{18''}$). MS (TOF-ES+) m/z: 888 (MH^+, 100%), 761 (MH^+-I, 97.95%), 496 (MH^+-CO-$C_{17}H_{34}I$, 12.18%). HRMS (MALDI matrix DHB) m/z: calcd ($C_{42}H_{83}INO_8P$, MH^+) 888.497, obsd. 888.497. FTIR: 2920 (s), 2851 (s), 1734 (s, C═O) 1466 (m), 1252 and 1091 (s, C−O and P═O), 967 (m, P−O−R-ester) 804 (w, C−I) cm^{-1}.

2.4.3.3. 1-Palmitoyl-2-(10′′-iodostearoyl)-sn-glycero-3-phosphatidylcholine (17c). 49.2% yield; ^{1}H NMR ($CDCl_3$): δ 5.20 (m, 1H,

Table 1
Summary of the fluorescence excitation (λ_{ex}) and emission (λ_{em})[a] wavelengths of compounds **1–5** within lipid bilayers.

Fluorophore	λ_{ex} (nm)	λ_{em} (nm) DMPC	λ_{em} (nm) Bioliposomes	λ_{em} (nm) Ghosts
PPn (**1**)	404	636	637	637
HPn (**1**)	404	624	625	626
Coumarin-314 (**3**)	436	491	492	487
Resorufin (**4**)	563	589	590	582
NBD (**5**)	460	540	539	527

[a] The emission maxima are somewhat sensitive to media and the exact derivative of compounds **6** and **7** used, thus varying slightly from sample to sample.

H_2), 4.39 (m, 1H, H_{1b}), 4.35 (m, 2H, H_4), 4.11 (m, 1H, H_{1a}), 3.96 (m, 3H, $H_{10''}$ and H_3), 3.87 (m, 2H, H_5), 3.39 (s, 9H, H_6), 2.29 (m, 4H, $H_{2'}$ and $H_{2''}$), 1.85 (m, 2H, $H_{9''}$), 1.68 (m, 2H, $H_{11''}$), 1.58 (m, 4H, $H_{8''}$ and $H_{12''}$), 1.52 (m, 2H, $H_{3''}$), 1.29, 1.28 and 1.26 (m, 44H, methylenes: $H_{3'}$-$H_{15'}$, $H_{4''}$, $H_{7''}$ and $H_{13''}$-$H_{17''}$), 0.88 (2 "t", 6H, J = 7 Hz, $H_{16'}$ and $H_{18''}$). ^{13}C NMR ($CDCl_3$): δ 173.51 and 173.11 ($C_{1'}$ and $C_{1''}$), 70.29 (d, Jcp = 7 Hz, C_4), 66.26 (d, Jcp = 6 Hz, C_5), 63.67 (d, Jcp = 5 Hz, C_2), 62.79 (C_1), 59.55 (d, Jcp = 4 Hz, C_3), 54.44 (C_6), 40.71 and 40.66 ($C_{9''}$ and $C_{11''}$), 34.75 ($C_{10''}$), 34.26 and 34.11 ($C_{2'}$ and $C_{2''}$), 31.90 and 31.82 ($C_{14'}$ and $C_{16''}$), 29.70, 29.67, 29.65, 29.54, 29.43, 29.35, 29.26, 29.22 and 29.18 (methylenes: C_4–$C_{13'}$, $C_{4''}$–$C_{7''}$ and $C_{13''}$–$C_{15''}$), 29.08 and 28.85 ($C_{8''}$ and $C_{12''}$), 24.90 and 24.87 ($C_{3'}$ and $C_{3''}$), 22.66 and 22.63 ($C_{15'}$ and $C_{17''}$), 14.09 and 14.08 ($C_{16'}$ and $C_{18''}$). MS (TOF-ES+) m/z: 888 (MH^+, 100%), 761 (MH^+-I, 14.72%), 496 (MH^+-CO-$C_{17}H_{34}I$, 1.15%). HRMS (MALDI matrix DHB) m/z: calcd ($C_{42}H_{83}INO_8P$, MH^+) 888.497, obsd. 888.497. FTIR: 2921 (s), 2851 (s), 1734 (s, C═O) 1466 (m), 1240 and 1061 (s, C—O and P═O), 969 (m, P—O—R-ester) 820 (w, C—I) cm^{-1}.

2.4.3.4. 1-Palmitoyl-2-(14''-iodostearoyl)-sn-glycero-3-phosphatidylcholine (17d). 57.3% yield; ^{1}H NMR ($CDCl_3$): δ 5.21 (m, 1H, H_2), 4.38 (m, 2H, H_4), 4.36 (m, 1H, H_{1b}), 4.13 (m, 2H, H_{1a} and $H_{14''}$), 4.00 (m, 2H, H_3), 3.91 (m, 2H, H_5), 3.40 (s, 9H, H_6), 2.29 (m, 4H, $H_{2'}$ and $H_{2''}$), 1.85 (m, 2H, $H_{13''}$), 1.69 (m, 2H, $H_{15''}$), 1.57 (m, 4H, $H_{12''}$ and $H_{16''}$), 1.50 (m, 2H, $H_{3''}$), 1.33 and 1.30 (m, methylenes: 44H, $H_{3'}$-$H_{15'}$, $H_{4''}$-$H_{11''}$ and $H_{17''}$), 0.91 ("t", 3H, J = 7 Hz, $H_{18''}$), 0.874 ("t", 3H, J = 7 Hz, H_{16}). ^{13}C NMR ($CDCl_3$): δ 173.51 and 173.15 ($C_{1'}$ and $C_{1''}$), 70.14 (d, Jcp = 6.5 Hz, C_4), 66.22 (d, Jcp = 6 Hz, C_5), 63.90 (d, Jcp = 3 Hz, C_2), 62.68 (C_1), 59.78 (d, Jcp = 3 Hz, C_3), 54.49 (C_6), 40.68 and 40.66 ($C_{13''}$ and $C_{15''}$), 34.28 and 34.10 ($C_{2'}$ and $C_{2''}$), 31.92 ($C_{14''}$), 31.67 ($C_{16''}$), 29.71, 29.66, 29.61, 29.55, 29.51, 29.36, 29.34, 29.27, 29.18 and 29.15 (methylenes: C_4–$C_{13'}$ and $C_{4''}$–$C_{11''}$), 28.88 ($C_{12''}$), 24.94 and 24.88 ($C_{3'}$ and $C_{3''}$), 22.68 and 21.96 ($C_{15'}$ and $C_{17''}$), 14.11 and 13.96 ($C_{16'}$ and $C_{18''}$). MS (TOF-ES+) m/z: 888 (MH^+, 100%), 832 (MH^+-C_4H_8, 7.02%)761 (MH^+-I, 8.11%). HRMS (MALDI matrix DHB) m/z: calcd ($C_{42}H_{83}INO_8P$, MH^+) 888.497, obsd. 888.498. FTIR: 2917 (s), 2849 (s), 1737 (s, C═O) 1467 (m), 1170 and 1053 (m, C—O and P═O), 970 (m, P—O—R-ester) 821 (w, C—I) cm^{-1}.

2.5. Preparation of DMPC liposomes, bioliposomes and erythrocyte ghosts

The procedure for the preparation of DMPC liposomes, biological liposomes and erythrocyte ghosts has recently been described by Afri et al. (2014a,b) and Afri et al. (2014c). In order to verify the existence of the synthetic liposomes in the solution, coumarin 314 (**3**, Ex: 436 nm, Em: 491 nm) was intercalated in turn into DMPC, biolipids and erythrocyte ghosts and analyzed under a fluorescence microscope (Axioimager). The resulting images (see Supplemental material, Figs. S-1 through S-3) confirmed the spherical shape of the various liposomes in the expected size ranges of 1–10 μm (Torchilin, 2006) and the presence of the intercalants in the liposomal bilayer.

2.6. Fluorescence quenching by bromophospholipids, and iodophospholipids, and aqueous KBr/ KI (respectively) within DMPC, biological liposomes and erythrocyte ghosts

2.6.1. DMPC liposomes

For the preparation of intercalated DMPC liposomal suspensions for fluorescence measurements, samples of DMPC (5 μmol) and fluorescent intercalants (0.05 μmol) taken from ethanol stock solutions, were mixed together in the same vial. The solvent was removed via nitrogen bubbling, and then under vacuum for at least 2 h. Saline phosphate buffer solution at pH 7.4 (PBS-N_3, 1 mL) was added to the vial, and the vial was vortexed for 15 min. This sample was used to determine the reference maximal fluorescence value for a given fluorophore located within the DMPC liposome under the test conditions (henceforth, background). For determining the relative fluorescence quenching induced by the various *n*-BrPCs and *n*-IPCs, 5 vials with samples of DMPC (2.5 μmol or 5 μmol for the background), and each of the *n*-BrPCs **14** or the *n*-IPCs **17** (2.5 μmol), was taken from DCM stock solution in turn, in addition to the fluorescent intercalant (0.05 μmol from the ethanol stock solutions). The substrates were mixed together, the solvents from each of the vials was then removed (by nitrogen bubbling and under vacuum) and buffer was added to each of the five vials, as mentioned above. After vortexing for 15 min, the solution in each vial consisted of multilamellar liposomes. The sample was taken for fluorescence measurements. Fluorescence spectra were measured at the λ_{ex} and λ_{em} values appearing in Table 1. The amount of quenching of the various compounds with each one of the halophospholipid quenchers **14** or **17** was determined. We also measured the influence on the fluorescence quenching of adding KBr to *n*-bromophospholipid **14** or KI to *n*-iodophospholipid **17** in the liposomal solutions. To this end, aqueous potassium salt (100 μL from a 2.6 M from PBS-N_3 stock solution) was allowed to diffuse into the above DMPC–intercalant liposomal solutions, and the fluorescence was measured under the same conditions as before. Note that same results were obtained when the liposomes solutions were sonicated and the unilamellar liposomes were examined (we did not study the effect of ionic strength on the depth of penetration and liposome structure).

2.6.2. Bioliposomes

The preparation of intercalated biological liposomal suspensions was similar to the DMPC preparation with two modifications: Because the biological solution also contains substantial protein, a twofold amount was taken from the stock solution. Furthermore, after 15 min of vortexing, the biological solutions were sonicated for 13 min to give unilamellar liposomes prior to the fluorescence measurements. The influence on the fluorescence quenching of adding the relevant potassium salt (KX) or the halophospholipid on the various fluorophores samples were measured as detailed with DMPC liposomes (Section 2.6.1).

2.6.3. Erythrocyte ghosts

To a screw top 50 mL conical tube containing white membrane dispersion (ca. 2 g; see Section 2.5 above), were added the fluorophore (1.75 μmol) and 20 mL KCl-N_3 solution at pH 7.2, and incubated on a shaker bath (220 rpm at 37 °C) for 1 h. The erythrocyte ghosts were washed twice with PBS-N_3 buffer by centrifugation at 22,000*g* for 20 min at 4 °C. Then, 6.5 mL of PBS-N_3 buffer was added and 1 mL of this diluted solution was placed into 6 new tubes. To each tube a different derivative of *n*-halophospholipid (2.5 μmol) **14** or **17** was added and the tubes were incubated on a shaker bath (220 rpm at 37 °C) for another hour. The fluorescence quenching influence of adding the relevant potassium salt (KX) or the halophospholipid on the various fluorophores samples was measured as detailed with DMPC liposomes (Section 2.6.1).

3. Results and discussion

3.1. Synthesis of n-halophospholipids quenchers

Our synthesis of halophospholipids **14** and **17** appears in Schemes 1 and 2, and begins with ketoesters **9**, whose synthesis has been recently described by Afri et al. (2014a). $NaBH_4$ reduction of ketoesters **9b–d** yields the corresponding *n*-hydroxyesters **10b–d** which were then converted with triphenylphospine dibromide to the matching bromoesters **11b–d**, or with triphenylphospine and iodine to the matching iodoesters **15b–d**. Barium hydroxide mediated the monohydrolysis of the latter to the desired *n*-bromostearic acid esters **12b–d** and *n*-iodostearic acid esters **16b–d**. 2-Bromopalmitic acid (**12a**) is commercially available, while the corresponding iodo-derivative **16a** (2-iodopalmitic acid) was prepared by halogen exchange of **12a** with sodium iodide. The final step was to esterify the haloacids with 1-palmitoyl-2-hydroxy-*sn*-glycero-3-phosphatidylcholine (lysoPC 16:0, **13**) yielding 1-palmitoyl-2-(*n*-bromostearyl)-*sn*-glycero-3-phosphatidylcholine (*n*-BrPSPC, **14b–d**) and 1-palmitoyl-2-(*n*-iodostearyl)-*sn*-glycero-3-phosphatidylcholine (*n*-IPSPC, **17b–d**). In the cases of **12a** and **16a**, the products were 1-palmitoyl-2-(2-bromopalmitoyl)-*sn*-glycero-3-phosphatidylcholine (2-BrPPPC, **14a**) and 1-palmitoyl-2-(2-iodopalmitoyl)-*sn*-glycero-3-phosphatidylcholine (2-IPPPC, **17a**).

All products were identified and characterized by their spectral data, most prominently NMR. In ^{1}H NMR, bromoesters **11** and iodoesters **15** have a distinctive sharp singlet at ca. 3.6 ppm for the methoxy ester protons and a multiplet at ca. 4 ppm for the proton geminal to the bromine or iodine (-C**H**X-R). ^{13}C NMR chemical shifts for the ester carbonyls are at approximately 174 ppm, while the brominated and iodinated carbons appear at approximately 58 and 40 ppm, respectively. The hydrolysis of esters **11** and **15** to the corresponding acids **12** and **16** was confirmed by the disappearance of the ester peak at 3.6 ppm, with a shift of the carbonyl carbon downfield to 180 ppm. The ^{1}H NMR of the hydrogen geminal to the bromine in the bromoesters or bromoacids was split into a quintet, while the analogous hydrogen geminal to the iodine was split into a septet. The difference in the observed splitting presumably results from the differing atomic size of the halogens and their influence on respective rotamers. (Kraszni et al., 2004)

The coupling of bromoacids **12** or iodoacids **16** with lysoPC **13** to form bromophospholipids **14** and iodophospholipids **17** was easily verified by the ^{1}H chemical shifts of the methylene protons H1–H5 [the numbering of the hydrogens and carbons in halophospholipids **14** and **17** is shown in Section 2.1 above]. As exemplified by 6-BrPSPC **14b** in Fig. 2, the most dramatic change occurs in H2, which moves downfield by ca. 1.25 ppm in this transformation. This is because carbon C2 goes from being adjacent to a hydroxyl group (a quintet at 3.95) in the starting material, to being adjacent to an ester moiety (multiplet at ca. 5.2 ppm) in the product. At the same time, one can detect a small concomitant upfield movement in H3–H5. The diasteriotopic protons H1a and H1b appear, respectively, at 4.12 and 4.18 ppm in lysoPC **13,** but at ca. 4.1 and 4.4 ppm in 6-BrPSPC **14b**.

3.2. Fluorescence quenching

3.2.1. Depth of halogens in n-haloPCs *14* and *17*

We have thus successfully synthesized brominated and iodinated phosphatidylcholines (*n*-BrPCs **14** and *n*-IPCs **17**), with the halogen atoms located on various carbons along the C2 lipid chain. Our ultimate goal is to incorporate these halogen moieties into phospholipid bilayer systems (DMPC liposomes, bioliposomes and erythrocyte ghosts) and use the heavy atom to quench fluorescent moieties. This quenching will occur most efficiently when the halogen of the haloPC **14** and **17** is in a proximate location to the fluorescent moiety. Thus, if we know the location of the halogen in the most efficiently quenching derivative, we can determine the approximate depth of the fluorescent moiety.

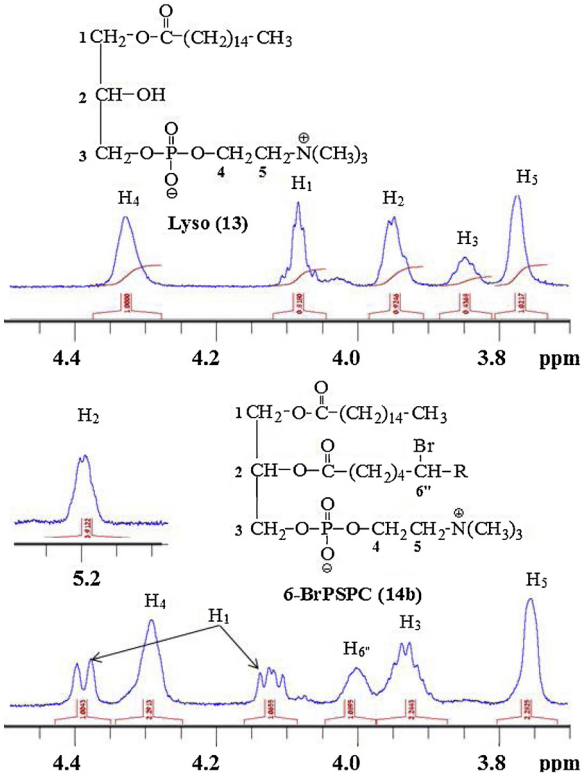

Fig. 2. Comparison of the ^{1}H NMR spectra of lysoPC (**13**) and 6-BrPSPC (**14b**).

In previous papers (Afri et al., 2014b; and c), we described an "NMR method," which allowed us to determine the depth (Angstrom distance from the lipid/water interface) of the keto moiety of *n*-ketoPCs **18** (Fig. 3) within three bilayer systems: DMPC liposomes, biomembranes and erythrocyte ghosts. As discussed above, this NMR method is based on the excellent correlation that exists between the ^{13}C chemical shifts of polarizable carbons (like the carbonyl) and solvent polarity.

Unfortunately, this NMR method is not directly applicable to *n*-haloPCs **14** and **17** because the brominated or the iodinated carbon is not particularly polarizable and, hence, no solvatochromism (i.e., solvent polarity dependence of chemical shift) exists. Nevertheless, since we have already determined the $E_T(30)$ depth of the comparable *n*-keto carbon in the corresponding *n*-ketoPC analog **18** (Cohen et al., 2008b; Afri et al., 2014b), it seems appropriate to assume that the *n*-halo carbon will essentially lie at the same depth. Assuming that the carbon chain is aligned vertically within the lipid bilayer, with the bromine or with the iodine substituent lying essentially horizontally to it, we can assign the same depth value as that of the carbon on which it is located. Afri et al. (2014b) have also developed a chemical ruler which correlates the measured $E_T(30)$ value with penetration depth (in Å) from the water-lipid interphase. This leads to the angstrom depth values for the bromine or iodine atoms in bromoPCs **14** or iodoPCs **17** given in Table 2 (X = Br/I). The water soluble KBr and KI salts were assigned a depth value of zero.

We should note that although the $E_T(30)$ value for ketoPCs **18a** (n = 2) and **18d** (n = 14) are not listed in Afri et al. (2014b), the n = 1 and n = 13 analogs do appear with the corresponding experimental $E_T(30)$ values of 50.4 and 34.4 kcal/mol. The corresponding calculated values for using Cohen's chemical ruler (Afri et al., 2014b) gives angstrom depth values of 3.75 and 18.5. Molecular modeling calculations (PCModel; Afri et al., 2014b) show that each C–C bond increases bilayer penetration by ca. 1.5 Å. This places ketoPCs **18a** (n = 2) and **18d** (n = 14) (and the corresponding haloPCs **14** and **17)** at 5.25 and 20 Å. Afri et al.'s chemical ruler gives the corresponding $E_T(30)$ values of 47.0 and 33.5 kcal/mol. These values appear in Table 2.

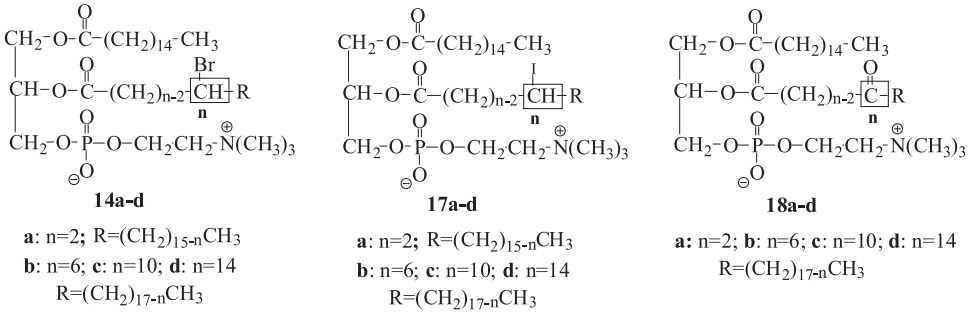

Fig. 3. The comparable structures of *n*-haloPCs **14** and **17** and *n*-ketoPCs **18**.

*3.2.2. Fluorescence quenching with n-bromoPCs **14** and with n-iodoPCs **17***

Fluorescence quenching measurements were carried out in three bilayers systems: DMPC liposomes, biomembranes and erythrocyte ghosts. *n*-HaloPC derivatives **14a–d** or **17a–d** were incorporated in turn within the various bilayers systems together with the various fluorophores **1–5**. The fluorescence emission of the latter was measured in each case. Fluorescence quenching graphs of PP3 (**1b**), HP9 (**2c**), coumarin 314 (**3**) and NBD (**5**) - by KBr, KI, bromophospholipids and iodophospholipids within DMPC liposomes, bioliposomes and erythrocyte ghosts are found in the Supplemental Material section of this paper. As expected, the maximum emission intensity was where the dyes were intercalated within halogen-free bilayers. The presence of a bromine or iodine atom on the haloPCs resulted in some quenching of the fluorescence emission, though the exact amount of quenching was decidedly dependent on the exact location of the halogen along the lipid chain. As noted above, the closer the heavy atom is to the dye molecule, the greater will be the decrease in the fluorescence emission. The various intercalated dyes are locating in different regions within the bilayers because of their differing polarity character. Thus, the hydrophilic fluorescent intercalants are located at or near the interface region of the membrane and their fluorescence is more effectively quenched by haloPCs whose bromine or iodine lies in more shallow areas of the membrane. We also observed that the very shallow lying intercalants are influenced by the water soluble fluorescence quenchers KBr and KI. The lipophilic intercalants, on the other hand, lie deeper between the hydrophobic chains of the membrane, and their fluorescence is essentially unaffected by KBr or KI. As expected, though, they are more efficiently quenched by haloPCs with the deeper situated halogen.

We will demonstrate the fluorescence quenching procedure for intercalated protoporphyrin PP3 (**1b**) within DMPC liposomes for the BrPC series. Protoporphyrins are fluorescent tetrapyrroles (widely used in photodynamic therapy) containing two alkylcarboxylate side chains. We assume that the very lipophilic porphyrin ring will gravitate toward the low polarity center of the bilayer, while the carboxylate end is anchored near the hydrophilic interface. The length of the alkylcarboxylate side chains determines the depth at which these molecules penetrate the lipid bilayer (see Fig. 1). PP3 has two such side chains, containing 3 methylenes between the ring and the carboxylate moiety. We also assume that the planar porphyrin ring is aligned parallel to the lipid chains causing only minimal perturbation to the liposomes. The PP3 dye was incorporated (in a 1:100 M ratio) within DMPC liposomes or within liposomes prepared from a 1:1 mixture of DMPC and *n*-BrPCs **14a–d**, as detailed in the experimental Section (2.6.1). In the latter case, we assume that the substitution of a single H or O, by a Br or I does not drastically change the polarity, shape or behavior of the very large lipid molecule.

The fluorescence of the two liposomal samples was measured under corresponding conditions (404 and 636 nm for PP3's excitation and emission wavelength, respectively), as appears in Table 1. As already noted at the bottom of Table 1, the emission maxima are somewhat sensitive to the substrate and media, and vary slightly from sample to sample. Since we are near or at the maxima, this variance has only a negligible effect on the fluorescence amplitude measured, as shown in Graph 1 .

Graph 1 presents the fluorescence of PP3 intercalated within DMPC liposomes in the absence and presence of free bromine ion (from KBr) or a bromine atom covalently connected to the lipid chain of various *n*-BrPCs **14a–d**. The results were normalized relative to the highest fluorescence of PP3 (**1b**) in DMPC liposomes in the absence of quenchers. Of the four *n*-BrPCs, we see that 6-BrPC (**14b**) was the best quencher of PP3 fluorescence with the fluorescence observed being 69% of that observed in the absence of quencher (31% quenching). Of the remaining *n*-BrPCs, 2-BrPC (**14a**) and 10-BrPC (**14c**) quenched PP3 with about the same efficiency (23% and 26% fluorescence, respectively) but better than KBr and 14-BrPC (**14d**) (only 14% and 9% quenching). These quenching results indicate that the center of the fluorophore of PP3 is located near the brominated carbon of 6-BrPC (**14b**). We then repeated this procedure with bioliposomes and erythrocyte ghosts, measuring the fluorescence in the absence and presence of KBr and *n*-BrPCs **14a–d**. The results revealed again that the PP3 fluorophore is located closest to 6-BrPC (**14b**), in all three bilayer systems (see below Table 3).

According to Table 2, this places PP3 at ca. 10 Å from the interface within DMPC liposomes. This value is not that far from our previous determination using London's Parallax method (Bronshtein et al., 2004), which placed this porphyrin at ca. 12.7 Å from the bilayer interface. Since the length of a DMPC molecule is ca 22 Å, this places PP3 more than half-way down the lipid. Again we see that overall the correspondence between the parallax method and our bromide quenching method is good.

We repeated the whole procedure with remaining protoporphyrins PP2 and PP7 and these results are also shown in Table 3. Again we see that overall the correspondence between the parallax method and our

Table 2
Approximate distance of the haloPC quenchers **14** and **17** from the water-lipid interphase of DMPC liposomal bilayers based on ketoPC analogs **18**.[a]

Quencher	KBr/KCl	n = 1	14a/17a n = 2	14b/17b n = 6	14c/17c n = 10	n = 13	14d/17d n = 14
$E_T(30)_{exp}$[a]	63.0	50.4		42.7	37.4	34.4	
$E_T(30)_{calc}$[b]	63.0	50.4	47.0	39.4	35.3	34.0	33.5
Distance (Å)	0	3.75	5.25	10	15.5	18.5	20

[a] kcal/mol.
[b] Afri et al. (2014b).

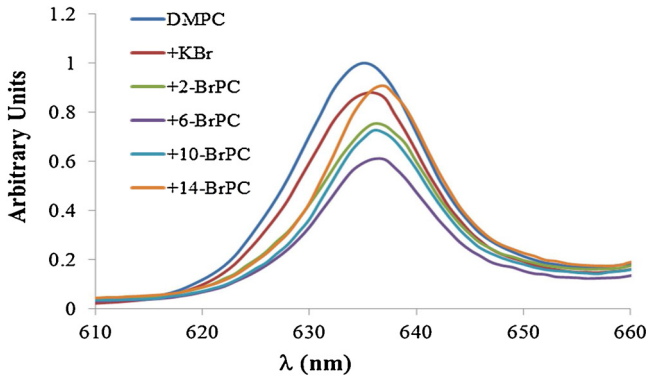

Graph 1. Fluorescence of PP3 (**1b**) within DMPC liposomal solutions with and without bromine quenchers.

bromide quenching method is good. But there is one serious discrepancy in the data. PP2 seems to intercalate deeper into the erythrocyte ghosts than it does into DMPC and bioliposomes. This might suggest that because of the various biomaterials located in the natural ghosts, the overall environment is more lipophilic supplying improved solvation of the lipophilic porphyrin end of the intercalant. This facilitates deeper penetration of latter into the bilayer. It is also possible that the proteins in this samples are also partially membrane penetrating and they are opening up spaces (disturbing head group packing) so that the fluorophores can penetrate deeper into the bilayer.

We used both bromophospholipids **14** and iodophospholipids **17** as quenchers. The disadvantage of the latter is that the iodine atom has a radius of 1.33 Å which is longer than that of bromine's 1.14 Å. As a result, iodine is less selective in the depth of the fluorescence molecules it will quench. In addition, the quenching of iodine is stronger than that of bromine, and thus the quenching effected by the iodophospholipids is more potent than that of the bromophospholipids). (Lindman and Forsen, 2012) Indeed, the spin-orbital constant of I is more than twice that of Br - with intersystem crossing highly distance dependent (Downs and Adams, 1973).

The results for the iodide quenchers **17a–d** appear to the right of Table 3. As we expected, iodide is much less discerning. Indeed, 6-IPC located (by NMR on the corresponding carbonyl) at 10 Å quenches PP2 and PP3 efficiently - ranging from 5.5 to 12.7 Å (parallax). Nevertheless, the highly lipophilic PP7 (**1c**) - located by parallax at 15 Å - is preferentially quenched by 10-IPC (**17c**) located at 15.5 Å [We do not understand the anomalous behavior of PP7 in erythrocyte ghosts, though - as noted for PP2 - above it may result from the proteins present in this samples.].

The results thus suggest that the bromoquenchers **14** give rather decent results for determining the depth of penetration of fluorescent intercalants into DMPC and bioliposomes.

We next explored the intercalation of hematoporphyrins **2a–c**. Unfortunately, Bronshtein et al. (2004) did not carry out parallax studies on this family of compounds. However, because of the overall similarity in structure to protoporphyrins **6**, we assumed that the results of penetration depth for **2a** (n = 2) and **2b** (n = 7) would be similar to those of the corresponding protoporphyrins **1a** (n = 2) and **1c** (n = 7). Thus in the results summarized in Table 4, under "Fluorophore Depth" we have inserted the depth value of the corresponding protoporphyrin determined by parallax.

Studying the results of Table 4 for the bromo-quenchers, the data again shows a good correlation between the location of the fluorophore and quencher. In addition our assumption that the various HPn derivatives correspond well to the PPn analogs seems justified. Indeed, there is one discrepancy in the data and that has to do with the location of HP2 in erythrocyte ghosts. As in the case of PP2 described above, HP2 seems to intercalate deeper into the erythrocyte ghosts than it does into DMPC and bioliposomes. As before, we attribute this to the various biomaterials located in the natural ghosts, which renders the overall environment more lipophilic. This, in turn, results in improved solvation of the lipophilic porphyrin end of the intercalant and facilitates deeper penetration of latter into the bilayer.

With these promising results, we attempted to extend these methods to another three intercalants, fluorophores **3–5** (see Fig. 1). The penetration of these fluorophores into the membrane of a DMPC liposome was previously determined in ***E*$_T$(30) values** (kcal/mol/) using the NMR method (Afri et al., 2014b). The corresponding Angstrom value (Å) was interpolated from these values using Cohen et al. (2008b) conversion table. Table 5 summarizes the results.

The data indicates that all three fluorophores **3–5** lie at or near the lipid water interface. These results jibe nicely with the quenching data effected by the bromo-quenchers. In the case of resorufin **4** which lies at the interface, KBR - which lies in the water phase is the most effective quencher. For the other two fluorophores which lie close to each other in the high polarity area of the membrane (more than 1 Å from the interface), 2-BrPC (**14a**) is the most effective quencher. The latter is estimated to also lie high up in the membrane (ca. 5 Å from the interface), though not as high as fluorophores **3** and **5.** (Again there is an inconsistency regarding the erythrocyte ghost data for NBD **5** which we are at a loss to explain.) In all three cases, KI quenched the fluorophores effectively. As already noted, the larger radius of iodine results in longer-distance and stronger quenching (Lindman and Forsen, 2012) – and much less discrimination based on intercalation depth within the bilayer. Clearly more work is called for in the case of more lipophilic fluorophores.

Scheme 3 represents a schematic model for the location of three molecules resorufin, PP3 and PP7 within the bilayers.

4. Conclusion

Over more than two decades, our group has been exploring various techniques for determining the depth of intercalants into the lipid

Table 3
Comparison of the Location of Protoporphyrin Fluorophores **1a–c** and that of the most effective HaloPC quenchers **14** and **17**.

Fluoro-phore	Fluorophore Depth (Å)[a]	Vesicle Type[b]	Most Effective Br-Quenchers	Quencher Depth (Å)[c]	Most Effective I-Quenchers	Quencher Depth (Å)
PP2 (**1a**)	3.0	DMPC	2-BrPC (**14a**)	5.25	6-IPC (**17b**)	10
		Bio	2-BrPC(**14a**)	5.25	6-IPC (**17b**)	10
		EG	6-BrPC (**14b**)	10	6-IPC (**17b**)	10
PP3 (**1b**)	12.7	DMPC	6-BrPC (**14b**)	10	6-IPC (**17b**)	10
		Bio	6-BrPC (**14b**)	10	6-IPC (**17b**)	10
		EG	6-BrPC (**14b**)	10	6-IPC (**17b**)	10
PP7 (**1c**)	15.0	DMPC	10-BrPC (**14c**)	15.5	10-IPC (**17c**)	15.5
		Bio	10-BrPC (**14c**)	15.5	10-IPC (**17c**)	15.5
		EG	10-BrPC (**14c**)	15.5	6-IPC (**17b**)	10

[a] Distance from DMPC liposome interface, determined by Parallax (Bronshtein et al., 2004).
[b] Based on location of corresponding carbonyl analog using NMR method (see text and Table 2).
[c] Bio – Biological liposome; EG – erythrocyte ghost.

Table 4
Comparison of the Approximate Location of Hematoporphyrin Fluorophores **2a-c** and that of the most effective HaloPC quenchers **14** and **17**.

Fluoro-phore	Fluorophore Depth (Å)[a]	Vesicle Type[b]	Most Effective Br-Quenchers	Br-Quencher Depth (Å)[c]	Most Effective I-Quenchers	I-Quencher Depth (Å)[c]
HP2 (**2a**)	[3]	DMPC	2-BrPC (**14a**)	5.25	6-IPC (**17b**)	10
		Bio	2-BrPC (**14a**)	5.25	6-IPC (**17b**)	10
		EG	6-BrPC (**14b**)	10	6-IPC (**17b**)	10
HP7 (**2b**)	[15]	DMPC	10-BrPC (**14c**)	15.5	10-IPC (**17c**)	15.5
		Bio	10-BrPC (**14c**)	15.5	6-IPC (**17b**)	10
		EG	10-BrPC (**14c**)	15.5	6-IPC (**17b**)	10
HP9 (**2c**)		DMPC	10-BrPC (**14c**)	15.5	10-IPC (**17c**)	15.5
		Bio	10-BrPC (**14c**)	15.5	10-IPC (**17c**)	15.5
		EG	10-BrPC (**14c**)	15.5	6-IPC (**17b**)	10

[a] Distance from DMPC liposome interface. Parallax experiments (Bronshtein et al., 2004) on the HPn derivatives were not performed. Estimated values based on the related PPn analogs.
[b] DMPC – DMPC Liposome; Bio – Biological liposome; EG – erythrocyte ghost.
[c] Based on location of corresponding carbonyl analog using NMR method (see text and Table 2).

Table 5
Comparison of the Approximate Location of Hematoporphyrin Fluorophores **3–5** and that of the most effective haloPC quenchers **14**.

Fluoro-phore	Fluorophore Depth in [E_T(30)] (Å)[a]	Vesicle Type[b]	Most Effective Br-Quenchers	Br-Quencher Depth (Å)[c]	Most Effective I-Quenchers	I-Quencher Depth (Å)[c]
Resorufin **4**	[63] (0)	DMPC	KBr	0	KI	0
		Bio	KBr	0	KI	0
		EG	KBr	0	KI	0
Coumarin **3**	[60] (1)	DMPC	2-BrPC (**14a**)	5.25	KI	0
		Bio	2-BrPC(**14a**)	5.25	KI	0
		EG	2-BrPC (**14a**)	5.25	KI	0
NBD **5**	[60] (1)	DMPC	2-BrPC (**14a**)	5.25	KI	0
		Bio	2-BrPC (**14a**)	5.25	KI	0
		EG	KBr	0	KI	0

[a] Distance from DMPC liposome interface is based on the E_t(30) value (kcal/mol) determined by the NMR method (Afri et al., 2014b). The corresponding Angstrom value (Å) was interpolated from these values using Cohen et al. (2008b).
[b] DMPC: DMPC liposome; Bio: biological liposome; EG: erythrocyte ghost.
[c] Based on the location of corresponding carbonyl analog using NMR method (see text and Table 2).

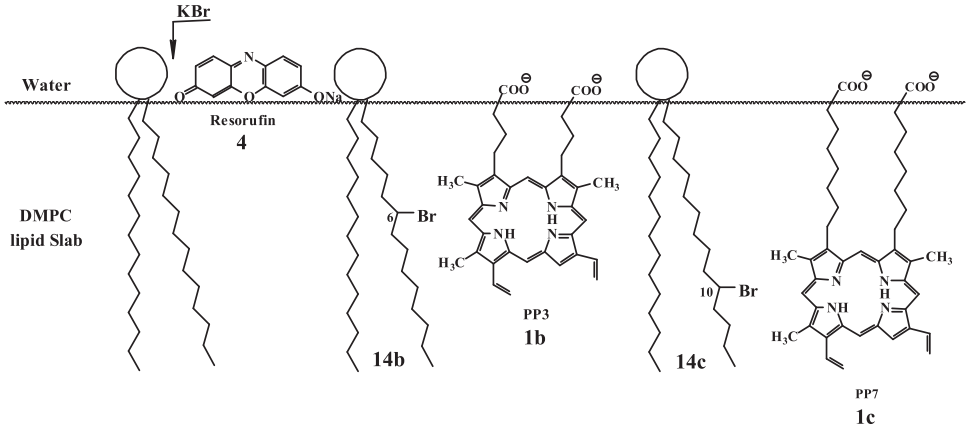

Scheme 3. Schematic model for the location of resorufin, PP3 and PP7 within liposomal bilayer using KBr and bromophospholipid quenching.

bilayer. In the present paper, we have been able to show the utility of a fluorescence quenching method - using bromophospholipids, **14** and iodophospholipids **17** to determine the location of fluorescent intercalants within DMPC liposomes, bio-liposomes and erythrocyte ghosts. We have demonstrated that the bromo-lipids **14** are substantially more discriminating than the iodo analogs. In addition, the intercalation depth results correspond favorably to previous data obtained using the "NMR method" and the "parallax fluorescence quenching" method.

Conflict of interest

There is no conflict of Interest.
Aryeh Frimer on behalf of all the authors.

Acknowledgements

This work was carried out as part of the Ph.D. research of Carmit Alexenberg at Bar Ilan University. We acknowledge the kind and generous support of the Ethel and David Resnick Chair in Active Oxygen Chemistry.

Appendix A. Supplementary data

Supplementary material related to this article can be found, in the online version, at doi:https://doi.org/10.1016/j.chemphyslip.2019.03.018.

References

Abrams, F.S., London, E., 1993. Extension of the parallax analysis of membrane penetration depth to the polar region of model membranes—use of fluorescence quenching by a spin-label attached to the phospholipid polar headgroup. Biochemistry 32, 10826–10831.

Afri, M., Gottlieb, H.E., Frimer, A.A., 2002. Superoxide organic chemistry within the liposomal bilayer. Part II: a correlation between location and chemistry. Free Radic. Biol. Med. 32, 605–618.

Afri, M., Ehrenberg, B., Talmon, Y., Schmidt, J., Cohen, Y., Frimer, A.A., 2004a. Active oxygen chemistry within the liposomal bilayer Part III: locating Vitamin E, ubiquinol and ubiquinone and their derivatives in the lipid bilayer. Chem. Phys. Lipids 131, 107–121.

Afri, M., Frimer, A.A., Cohen, Y., 2004b. Active oxygen chemistry within the liposomal bilayer Part IV: locating 2',7'-dichlorofluorescein (DCF), 2',7'-dichlorodihydrofluorescein (DCFH) and 2',7'-dichlorodihydrofluorescein diacetate (DCFH-DA) in the lipid bilayer. Chem. Phys. Lipids 131, 123–133.

Afri, M., Naqqash, M.E., Frimer, A.A., 2011. Using fluorescence to determine the depth of intercalants within the lipid bilayer of liposomes, bioliposomes and erythrocyte ghosts. Chem. Phys. Lipid 164, 759–765.

Afri, M., Alexenberg, C., Aped, P., Bodner, E., Cohen, C., Eigenberg, M., Eliyahu, S., Gilinsky-Sharon, P., Harel, Y., Naqqash, M.E., Porat, H., Ranz, A., Frimer, A.A., 2014a. NMR-based molecular ruler for determining the depth of intercalants within the lipid bilayer. Part III: studies on keto-esters and acids. Chem. Phys. Lipid 105–118.

Afri, M., Alexenberg, C., Aped, P., Bodner, E., Cohen, C., Eigenberg, M., Eliyahu, S., Gilinsky-Sharon, P., Harel, Y., Naqqash, M.E., Porat, H., Ranz, A., Frimer, A.A., 2014b. NMR-based molecular ruler for determining the depth of intercalants within the lipid bilayer. Part IV: studies on ketophospholoipids. Chem. Phys. Lipid 119–128.

Afri, M., Alexenberg, C., Bodner, E., Frimer, A.A., Jacob, A.I., Naqqash, M.E., 2014c. NMR-based molecular ruler for determining the depth of intercalants within the lipid bilayer. Part V, A comparison of liposomes, bioliposomes and erythrocyte ghosts. Chem. Phys. Lipid 184, 52–60.

Albrechtsen, S.E., 2006. Testing Methods for Seed-transmitted Viruses: Principles and Protocols. CABI Publishing, Wallingford, UK pp. 247 Appendix 2.

Balachander, N., Sukenik, C.N., 1990. Monolayer transformation by nucleophilic substitution: applications to the creation of new monolayer assemblies. Langmuir 6, 1621–1627.

Bodner, E., Afri, M., Frimer, A.A., 2010. Determining radical penetration into membranes using ESR splitting constants. Free Radic. Biol. Med. 49, 427–436.

Bronshtein, I., Afri, M., Weitman, H., Frimer, A.A., Smith, K.M., Ehrenberg, B., 2004. Porphyrin depth in lipid bilayers as determined by iodide and parallax fluorescence quenching methods and its effect on photosensitizing efficiency. Biophys. J. 87, 1155–1164.

Chattopadhyay, A., London, E., 1987. Parallax method for direct measurement of membrane penetration depth utilizing fluorescence quenching by spin-labeled phospholipids. Biochemistry 26, 39–45.

Cohen, Y., Bodner, E., Richman, M., Frimer, A.A., 2008a. NMR-based molecular ruler for determining the depth of intercalants within the lipid bilayer. Part I: discovering the guidelines. Chem. Phys. Lipids 155, 98–113.

Cohen, Y., Afri, M., Frimer, A.A., 2008b. NMR-based molecular ruler for determining the depth of intercalants within the lipid bilayer. Part II: quantitative values. Chem. Phys. Lipids 155, 114–119.

Cohen, Y., Afri, M., Frimer, A.A., 2008c. Aggregate formation in the intercalation of long chain fatty acid esters into liposomes. Chem. Phys. Lipids 155, 120–125.

Cudmore, A.J., Bradshaw, J.P., Alecio, M.R., 1994. X-ray diffraction studies using a novel synthetic phospholipids. Biophys. Chem. 49, 71–76.

Dimroth, K., Reichardt, C., Siepmann, T., Bohlmann, F., 1963. Pyridinium N-phenolbetaines and their use for the characterization of the polarity of solvents. Justus Liebigs Ann. Chem. 661, 1–37.

Downs, A.J., Adams, C.J., 1973. Pergamon texts in inorganic chemistry. The Chemistry of Chlorine, Bromine, Iodine and Astatine, vol. 7 Pergamon, Oxford see especially p. 1158.

Ervithayasuporn, V., Pornsamutsin, N., Prangyoo, P., Sammawutthichai, K., Jaroentomeechai, T., Phurat, C., Teerawatananond, T., 2013. One-pot synthesis of halogen exchanged silsesquioxane: octakis(3-bromopropyl)-octasilsesquioxane and octakis(3-iodopropyl)-octasilsesquioxane. Dalton Trans. 42, 13747–13753.

Frimer, A.A., Strul, G., Hameiri-Buch, J., Gottlieb, H.E., 1996. Can superoxide organic chemistry be observed within the liposomal bilayer? Free Radic. Biol. Med. 20, 843–852.

Gregoriadis, G., 1984. Liposome Technology Vol. I-III CRC Press, Boca Raton, FL.

Kachel, K., Asuncion-Punzalan, E., London, E., 1995. Anchoring of tryptophan and tyrosine analogs at the hydrocarbon polar boundary in model membrane liposomes: parallax analysis of fluorescence quenching induced by nitroxide-labeled phospholipids. Biochemistry 34, 15475–15479.

Kraszni, M., Szakacs, Z., Nosal, B., 2004. Determination of rotamer populations and related parameters from NMR coupling constants: a critical review. Anal. Bioanal. Chem. 378 (6), 1449–1463.

Lindman, B., Forsen, S., 2012. Chlorine, Bromine and Iodine NMR: Physico-Chemical and Biological Applications. Springer-Verlag, Berlin-Heidelberg-New York.

London, E., Feigenson, G.W., 1981. Fluorescence quenching in model membranes. An analysis of the local phospholipid environments of diphenylhexatriene and gramicidin A. Biochim. Biophys. Acta 649, 89–97.

Markello, T., Zlotnick, A., Everett, J., Tennyson, J., Holloway, P.W., 1985. Determination of the topography of cytochrome B5 in lipid vesicles by fluorescence quenching? Biochemistry 24, 2895–2901.

McIntosh, T.J., Holloway, P.W., 1987. Determination of the depth of bromine atoms in bilayers formed from bromolipid probes. Biochemistry 26, 1783–1788.

Meiresonne, T., Mangelinckx, S., Kimpe, N.D., 2012. Stereoselective synthesis of both enantiomers of trans-2-(diphenylmethylideneamino)cyclopropanecarboxylic acid using a chiral pool approach and their incorporation in dipeptides. Tetrahedron 68 (47), 9566–9571.

Menger, F.M., Richardson, S.N., Wood Jr., M.G., Sherrod, M.J., 1989. Chain-substituted lipids in monomolecular films. Effect of polar substituents on molecular packing. Langmuir 5, 833–838.

Papahadjopoulos, D., 1978. Liposomes and Their Uses in Biology and Medicine. Academy of Sciences, New York.

Reinert, J.C., Lowry, R.R., Wickman, H.H., 1977. Synthesis of a monobrominated analog of dipalmitoyl lecithin. Lipid 13, 85–87.

Shachan-Tov, S., Afri, M., Frimer, A.A., 2010. A reinvestigation of the reaction of coumarins with superoxide in the liposomal bilayer: correlation between depth and reactivity. Free Radic. Biol. Med. 49, 1516–1521.

Tanaka, A., 1959. Anodic synthesis of fatty acids. IV. Synthesis of chemical constituents of Conifer wax. Yakugaku Zasshi 79, 1327–1331 Cited by *Chem. Abstr.* 1960, 54, 4381d.

Tennyson, J., Holloway, P.W., 1986. Fluorescence studies of cytochrome B5 topography. J. Biol. Chem. 261, 14196–14200.

Torchilin, V., 2006. Adv. Drug Deliv. Rev. 58 (14), 1532–1555.

Tulloch, A.P., 1978. Carbon 13 NMR spectra of all the isomeric methyl hydroxy- and acetoxyoctadecanoates. Determination of chemical shifts by deuterium isotope effects. Org. Magn. Reson. 11, 109–115.

Wiener, M.C., White, S.H., 1991. Transbilayer distribution of bromine in fluid bilayers containing a specifically brominated analogue of dioleoylphosphatidylcholine. Biochemistry 30, 6997–7008.

Wiley, G.A., Hershkowitz, R.L., Rein, B.M., Chung, B.C., 1964. Organophosphorus chemistry. I. Conversion of alcohol and phenols to halides by tertiary phosphine dihalides. J. Am. Chem. Soc. 86, 964–965.